Scientific Reports
https://doi.org/10.1038/s41598-026-61687-0
Article in Press

Design and Optimization of AlGaN/GaN Graded Barrier MOS-HEMT Biosensor for Breast Cancer Biomolecule detection

Received: 10 April 2026

Accepted: 7 July 2026

Published online: 19 July 2026

Cite this article as: Karumuri S.R., Prasanna R.L., Sreenivasulu V.B. *et al.* Design and Optimization of AlGaN/GaN Graded Barrier MOS-HEMT Biosensor for Breast Cancer Biomolecule detection. *Sci Rep* (2026). https://doi.org/10.1038/s41598-026-61687-0

Srinivasa Rao Karumuri, Rudra Lakshmi Prasanna, Vakkalakula Bharath Sreenivasulu & Girija Sravani Kondavitee

Design and Optimization of Graded AlGaN Barrier MOS-HEMT Biosensor for Breast Cancer Biomolecule Detection

Srinivasa Rao Karumuri[1], Rudra Lakshmi Prasanna[1], V Bharath Sreenivasulu[2], Girija Sravani Kondavitee[1]

[1]VLSI-Microelectronics Research Lab, Department of Electronics and Communication Engineering, Koneru Lakshmaiah Education Foundation (Deemed to be University), Green Fields, Vaddeswaram, Andhra Pradesh, India.
[2] Department of Electronics and Communication Engineering, Manipal Institute of Technology Bengaluru, Manipal Academy of Higher Education, Manipal, Karnataka 576104, India.

Corresponding Author: Srinivasa Rao Karumuri (srinivasakarumuri@gmail.com); V. B. Sreenivasulu (vb.sreenivasulu@manipal.edu)

Abstract-: In this paper, we have designed and simulated an AlGaN/GaN graded barrier metal oxide semiconductor high electron mobility transistor (MOS-HEMT) heterojunction biosensor for detection of Breast Cancer biomolecules. A graded AlGaN barrier layer is utilized to enhance polarization-induced charges, thus increasing the density of 2DEG and improving carrier mobility in the channel. The proposed device uses Triple Metal Gate (TMG) with different work functions (M1, M2, M3) for controlling the electric field profile along the channel and improves the electrostatic control of the proposed biosensor. AlGaN graded barrier MOS-HEMT heterojunction biosensor was evaluated using Silvaco TCAD. The performance of proposed device analyzed using healthy breast cancerous biomolecules (K=4.5(MCF-10)) and non-healthy breast cancerous biomolecules (K=22(Hs578T), 27.5(MCF-7), 32(T47D)). The device characteristics are evaluated through transfer characteristics (I_d-V_{gs}), output characteristics (I_d-V_{ds}), electron(e^-) mobility and surface potential. Moreover, the effect of different positions for cavity fillings on I_{on}/I_{off} ratio sensitivity and V_{th} sensitivity is examined under different conditions. The sensitivity of the device is 0.147×10^2, subthreshold swing (SS) value is 60mV/dec, I_{on}/I_{off} ratio sensitivity is 3.67×10^5 at K=32. The results reveal that the sensitivity of the biosensor is based on the number of biomolecules rather than their position. The proposed biosensor has a relatively higher sensitivity compared to existing biosensors, making it a promising device for detecting Breast Cancer biomolecules.

Keywords: Biosensor, Graded barrier, 2DEG, HEMT, Sensitivity.

I. Introduction

Cancer is a major health problem in the world and it is one of the major causes of death. It is caused by changes in the genes, which affect the functioning of the cell, thereby causing uncontrolled cell growth and this is known as cancer. Cancers are mainly classified according to their origin and the type of cell from which they develop. Among them, Breast Cancer is the most common type of cancer in women, which is a major health problem. In the year 2025, it is expected to be the most common type of cancer in women, with a large number of new cases being reported each year. Additionally, the number of deaths due to the

Breast Cancer will be around 6,70,000 per year. Globally, Breast Cancer has been an important health concern among females. The incidence of the disease has been gradually increasing among females. It has been estimated that about 1 out of every 20 females could develop the disease during their lifetime. However, the detection of the disease in the early stages will be of great importance in the effective treatment of the disease. The survival probability of the patients who have been diagnosed with the disease will be about 99% [1]. Conventional diagnostic tools such as the use of the mammography method, MRI scans and ultrasonography are being employed to detect the disease, the tools are generally associated with low sensitivity and a higher cost of operation. In this scenario, microwave imaging utilizing variations in dielectric properties between cancerous (MCF-7) and normal (MCF-10A) breast cells has emerged as a promising approach for early Breast Cancer detection through dielectric modulation techniques. Among various methods of electrical sensing, FET-based biosensors have been recognized to be of significant interest owing to their high sensitivity, compactness, simplicity of use and cost-effectiveness[2-6]. Silicon-based FET biosensors have advantages such as compatibility with CMOS technology and control of device performance[7]. Nevertheless, biosensors have limited use under harsh conditions such as high temperature, high pressure and chemically reactive conditions [8]. Therefore, there exists a need for biosensors that are highly sensitive, reliable and scalable.

In this regard, AlGaN/GaN HEMT-based biosensors have been recognized to be of significant interest as an alternative solution to overcome the limitations of FET-based biosensors. This is due to the fact that the existence of a high mobility 2DEG at the heterointerface allows efficient charge transport. The proximity of the 2DEG channel to the surface of the device ensures that it is highly responsive to changes in charge at the surface, which is of great importance for biosensing applications. Furthermore, the chemical and thermal stability of GaN ensures reliable device performance even under harsh conditions[9-15]. Consequently, GaN HEMT device technology has been extensively used to sense a wide range of applications, such as pH sensing, gas/polar liquid sensing, as well as the identification of various biomarkers such as cardiovascular markers, C-reactive protein, breast-specific antigens and prostate-specific antigens. The previous works have reported the usefulness of GaN HEMTs for various sensing applications [16-21]. The sensing mechanism of the conventional HEMT biosensor to charged target biomolecules is a change in surface charge and surface potential. However, the detection of neutral biomolecules using GaN-based heterojunction devices are rare. In fact, different to charged biomolecules, to introduces a neutral biomolecules in sensing region induces a change in the overall capacitance characteristics of the MOS-HEMT device. This alteration in capacitance engenders variations in the surface potential and carrier concentration in the channel. Due to the change in capacitance, there will be a change in surface potential, which will further lead to a change in the carrier concentration, thus changing the output current. In earlier studies, MOS-HEMT has been used for the detection of neutral biomolecules [22-24]. In order to enhance the sensing properties of GaN-based MOS-HEMT biosensors, different optimization techniques have been proposed. In one study, a dual-channel MOS-HEMT has been used, which resulted in an improvement of sensitivity by about 74% [25-26], while dual-gate structures were proposed to optimize the sensing potential. The dual-gate MOS-HEMT increased the current for biotin by 78% compared with the single-gate device[27-28]. Nevertheless, the sensitivity of MOS-HEMT biosensors is still relatively low.

From the literature, the conventional graded HEMT face few challenges like high SS, low sensitivity and I_{on}/I_{off} ratio, to improve these parameters, we have proposed a MOS-HEMT heterojunction structure with graded AlGaN barrier layer and AlGaN/GaN heterostructures, the graded AlGaN barrier layer can form 2DEG layer. In addition, several novelties included use of unique work function for gate metals, HfO_2 as high-k dielectric gate oxide and device scaling for better design. The triple gate with different metals improves carrier transport and minimize leakage [29-32]. The characteristics of the proposed device is analyzed through transfer characterstics(I_d-V_{gs}), output characterstics (I_d-V_{ds}), electron concentration, electron(e^-) mobility and potential characteristics. Furthemore, the proposed AlGaN/GaN based MOS-HEMT analyzed the effect of biomolecules, thickness of AlGaN, Al mole fraction variation, sensitivity analysis, temperature analysis, cavity filling and steric hindrance issues. The proposed device has shown sensitivity of $0.147\text{x}10^2$ along with a subthreshold swing (SS) value of 60 mV/dec, this shows that this device is suitable for biosensing applications. The AlGaN/GaN graded barrier MOS-HEMT heterojunction based biosensor device is evaluated by considering the drain current and sensitivity for various biomolecules. The study has been done by considering MCF-10A cells as a healthy breast cell line with K = 4.5. In this study, Hs578T cells with K = 22, MCF-7 cells with K = 27.5, T47D cells with K = 32 are taken as cancerous breast cells. These cells are taken at 0.9 GHz under both neutral and charged conditions [30]. Moreover, the device performance has been simulated at the device level using the ATLAS tool. The study includes a healthy breast cell line i.e., MCF-10A (K = 4.5) and cancerous cell lines i.e., Hs578T (K = 22), MCF-7 (K = 27.5), T47D (K = 32) of breast tissue at 0.9 GHz for both neutral and charged conditions [30]. The performance of the proposed device is also simulated and evaluated at the device level using the ATLAS TCAD simulator.

This paper organized as the following: In Section II, the configuration of the device, simulation and fabrication, along with flowchart representation will be described. In Section III, the results will be presented and the electrical and sensing characteristics of the device will be analyzed. In Section IV, concluding remarks with future directions will be provided.

II. Proposed Device Structure and its Simulation

This section introduces the proposed biosensor that uses a GaN channel along with a graded AlGaN barrier to allow for fast, label-free and sensitive detection of Breast Cancer biomolecules. The GaN channel will act as a conduction channel and the graded AlGaN barrier will allow for the generation of a high-density 2DEG at the interface to facilitate efficient charge transport between the source and drain electrodes. A nanocavity will be placed between these electrodes to hold the target biomolecules. Detection will be performed by observing changes in the electric field resulting from the dielectric properties of the target biomolecules, which will be reflected as changes in I_d-V_{gs} characteristics.

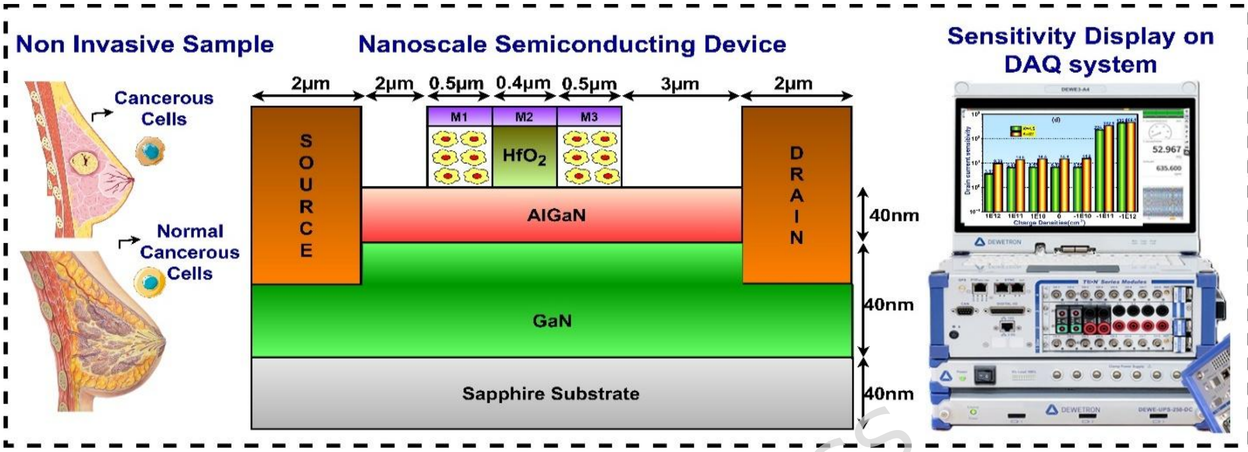

Figure.1 The 2D schematic view of Proposed MOS-HEMT heterojunction Biosensor

TABLE I
Simulation Parameters and Device Dimensions

Parameter	Values
Gate Length (M1,M2 and M3)	0.5 µm,0.4 µm, and 0.5µm
Source/Drain Length	2µm
Distance B/W source to gate	2µm
Distance B/W srain to gate	3µm
Width of AlGaN	40nm
Width of GaN	3µm
Width of sapphire substrate	3µm
Cavity thickness(C_t)	10nm
Cavity length (C_l)	0.5µm
Work functions of gate metals (M1, M2 and M3)	5.5eV, 4.9eV, and 4.5eV
Work functions of source and drain metals	3.93eV
Positive charge densities (q_f)	+1E12,+1E11,+1E10
Negative charge densities (q_f)	-1E12,-1E11,-1E10
Healthy Breast Cancer Biomolecule	K=4.5(MCF-10A)
Breast Cancerous Biomolecules	K=22(Hs578T), K=27.5(MCF-7), K=32(T47D)
Other Biomolecules	K=8(Keratin), K=12(Gelatin)
Polar scale	0.8
Temperature (T)	200K,300K,400K
Models	srh, fermi, bgn, conmob,cvt, albrct.n
Gate to source voltage(V_{gs}) / constant V_{ds}= -2V	-2V to 5V
Drain to source voltage(V_{ds}) / constant V_{gs}=2V	0V to 20V

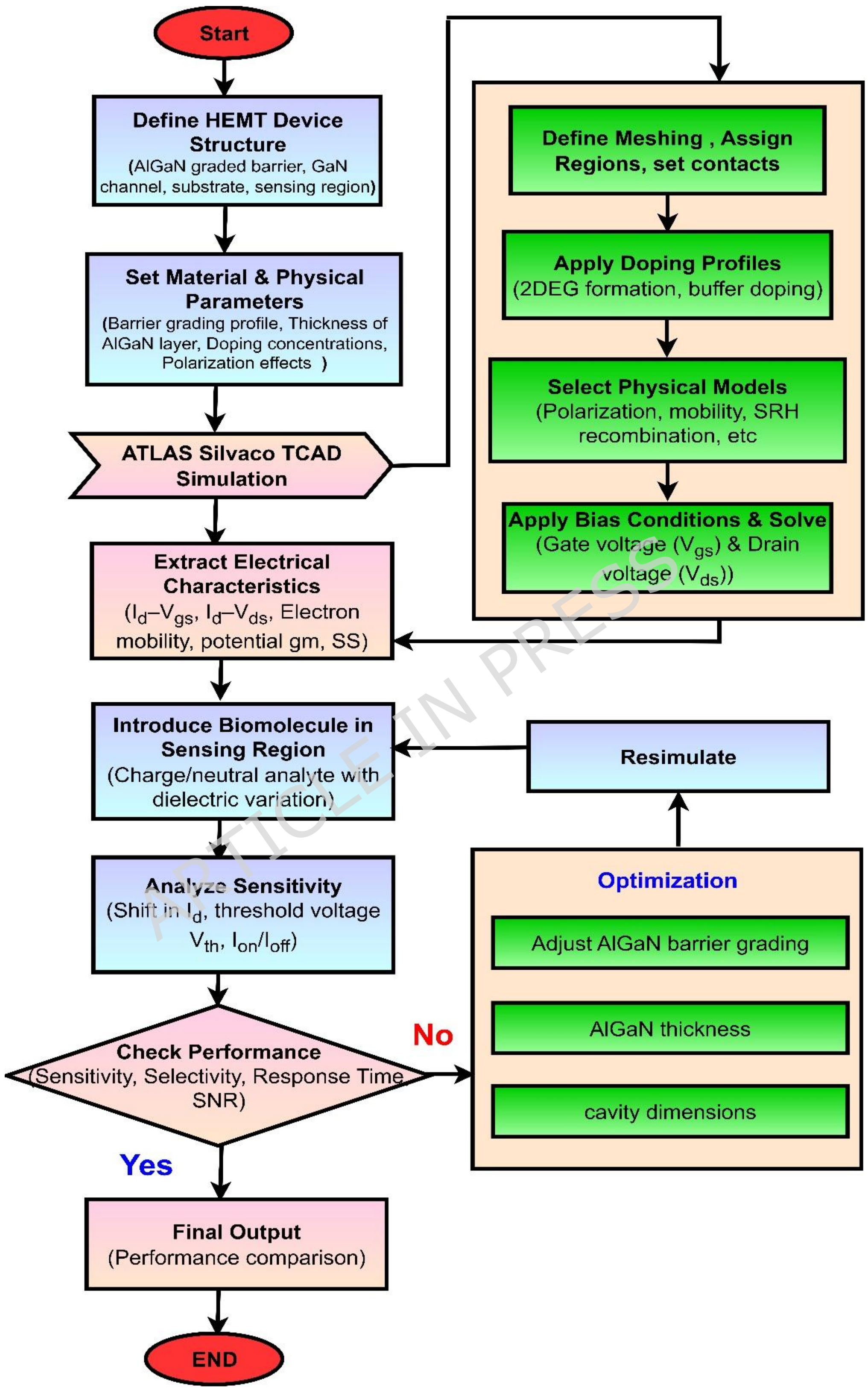

Figure.2 SILVACO ATLAS TCAD Flow for Proposed MOS-HEMT heterojunction Biosensor

The proposed device fabricated with a 40 nm thick AlGaN barrier layer to increase the efficiency of operation on a sapphire substrate. To achieve improved electrostatic control, three different metal work function gates M1, M2 and M3 are used in the channel region to control the electric field. The spacing between gate-source and gate-drain are set to be asymmetric to increase the injection efficiency from the source region and minimize short-channel effects. The device used a graded LGAN barrier with gradual variation in the dielectric material along the thickness of the barrier is shown in Figure. 1. Furthermore, the use of HfO_2 as the gate dielectric near the cavity region, which helps to achieve effective electrostatic interaction between the gate and the channel. The HfO_2 based device achieves Subthreshold swing of 60mV/dec while preserving high sensing performance. The electric field is enhanced due to the high value of the dielectric constant, thereby improving both the sensitivity and stability of the device while detection. Moreover, scaling is achieved by optimizing the parameters, which include cavity length (C_l), cavity thickness (C_t) and the materials used in the dielectric. The above parameters are optimized to improve the overall sensing device. The Table I shows the device parameters to design the proposed device.

In this work, the biosensor properties of AlGaN/GaN graded barrier MOS-HEMT heterojunction biosensors by introducing different target biomolecules in regions I and II are observed Atlas silvaco TCAD simulations. The simulations are carried out using the newton iterative method. The simulation of the AlGaN/GaN graded barrier MOS-HEMT heterojunction biosensor is carried out by incorporating important physical models like polarization, Fermi-Dirac, Shockley-Read-Hall (SRH) recombination and low-field mobility. The accurate representation of the device is achieved by incorporating these models and their detailed descriptions are provided in the supplementary material. Numerical calculations are performed using Fermi-Dirac statistics. GaN, AlGaN and HfO_2 are used from the built-in material database in TCAD simulations. Figure. 2 shows the flowchart of the proposed structured representation of the overall simulation and sensing scheme of the proposed AlGaN/GaN graded barrier MOS-HEMT heterojunction biosensor from the design of the device to the analysis of the device performance. The simulation, characterization, and interaction of the biosensor with the biomolecules are integrated in the flowchart, along with the optimization of the parameters for the improvement of the efficiency of the biosensor device. The tentative fabrication process of the proposed AlGaN/GaN graded barrier MOS-HEMT heterojunction biosensor is shown in Figure. 3. The fabrication process begins with a substrate made of sapphire. This is chosen because of its high thermal stability and the potential to use it in growing a GaN-based epilayer. The process begins with RCA cleaning of the substrate that removes any impurities from its surface and prepares it for epitaxy with quality results. The deposition of the GaN buffer layer by MOCVD technique and then deposition of the AlGaN barrier layer with graded aluminum composition. This gradient barrier increases the polarization effect at the AlGaN/GaN interface, resulting in creation of a high density of the

2DEG channel. After the completion of the epitaxial growth steps, the photolithographic process is utilized to create the source and drain areas on the semiconductor layer. The ohmic contacts can be fabricated by means of metal deposition and rapid thermal annealing to achieve low contact resistance. A high-k HfO_2 dielectric layer can be deposited using the ALD technique for enhancing electrostatic coupling between the gate and the channel, providing better control of the channel.The nanocavity region is achieved through lithography and reactive ion etching (RIE) to obtain a region for immobilizing of Breast Cancer biomolecules. The gate electrode is achieved through metal evaporation and deposition techniques using metals such as Pt/Ni/Au to achieve a graded barrier MOS-HEMT heterojunction biosensor device.

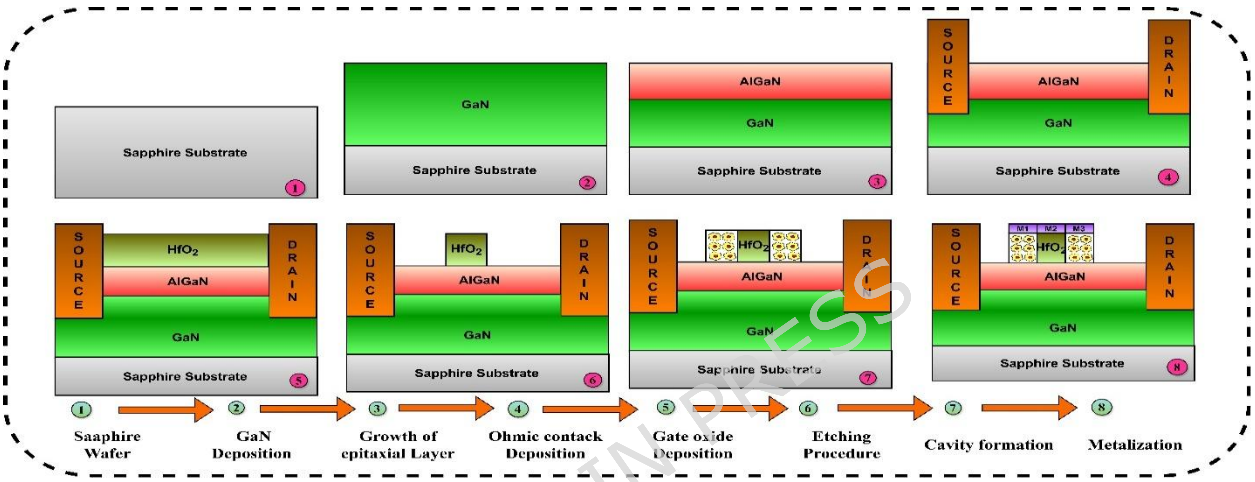

Figure.3 Tentative fabrication Flow

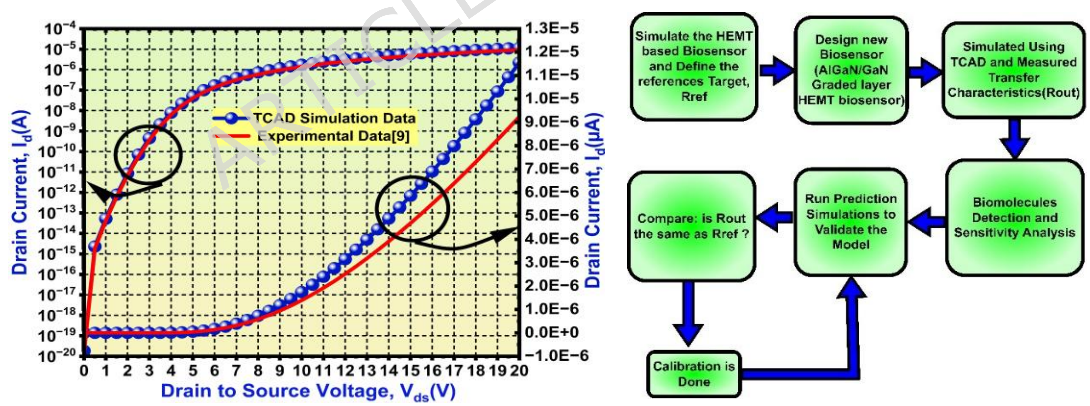

(a) (b)

Figure.4. (a) Calibration of simulation model with experimental data [9]. (b) Flowchart of simulation model.

The TCAD simulation model was first verified by comparing the simulated drain current with experimentally published values, as shown in Figure. 4(a). The correlation between the simulation and experiment results validates the use of the chosen physical models and parameters for the devices. The validated TCAD model was used to design the proposed graded barrier AlGaN/GaN MOS-HEMT heterojunction biosensor for the calibration process which is shown in Figure. 4(b).

III. Results and Discussions

In this section, the physical and electrical characteristics of the proposed AlGaN/GaN graded barrier MOS-HEMT heterojunction biosensor device are discussed. Various parameters are discussed in this section, including AlGaN thickness variation, change in Al mole fraction, and gate engineering. A comparative analysis is also provided for the conventional and graded barrier heterostructures. The effects of the length and thickness of the cavity are also discussed in this section. Moreover, the effect of biomolecules on the device is examined. This includes the response of the device to both neutral and charged biomolecules that are placed into the cavity region. The temperature-dependent characteristics of the device are examined to assess the proposed biosensor performance under varying temperature conditions. Additionally, the effect of steric hindrance, such as cavity filling factor on device performance is examined to understand the effect of the concentration of biomolecules within the cavity.

A. Effect of AlGaN Thickness and Its Mole Fraction

The effect of the AlGaN barrier layer thickness on the proposed biosensor is analyzed to find an optimal value for better electrical characteristics. The device is simulated for different values of AlGaN barrier layer thicknesses: 20 nm, 30 nm and 40 nm, with a constant dielectric constant K = 32 and the presence of neutral biomolecules with zero fixed charge density (q_f= 0) in a typical barrier HEMT structure. The transfer characteristics (I_d-V_{gs}) in Figure. 5(a) shows that the drain current increases with increasing AlGaN thickness due to the increased electric field and the corresponding increase in the concentration of the two-dimensional electron gas (2DEG) channel. The output characteristics (I_d-V_{ds}) in Figure. 5(b) shows that the drain current increases with increasing AlGaN barrier layer thickness. This is due to the increased confinement of the carriers in the channel, which causes a decrease in the scattering and an increase in the efficiency of the carrier transport from the source to the drain. The electron mobility(e- mobility) profile indicates that the maximum mobility occurs at the AlGaN/GaN interface, where 2DEG channel forms.
Figure. 5(c) shows that the 40 nm thick AlGaN barrier has a slightly higher electron mobility because the stronger polarization field provides better carrier confinement. The potential distribution along the device depth is shown in Figure. 5(d). A 40 nm thick AlGaN barrier has a smoother potential gradient, providing better electrostatic control in the channel.

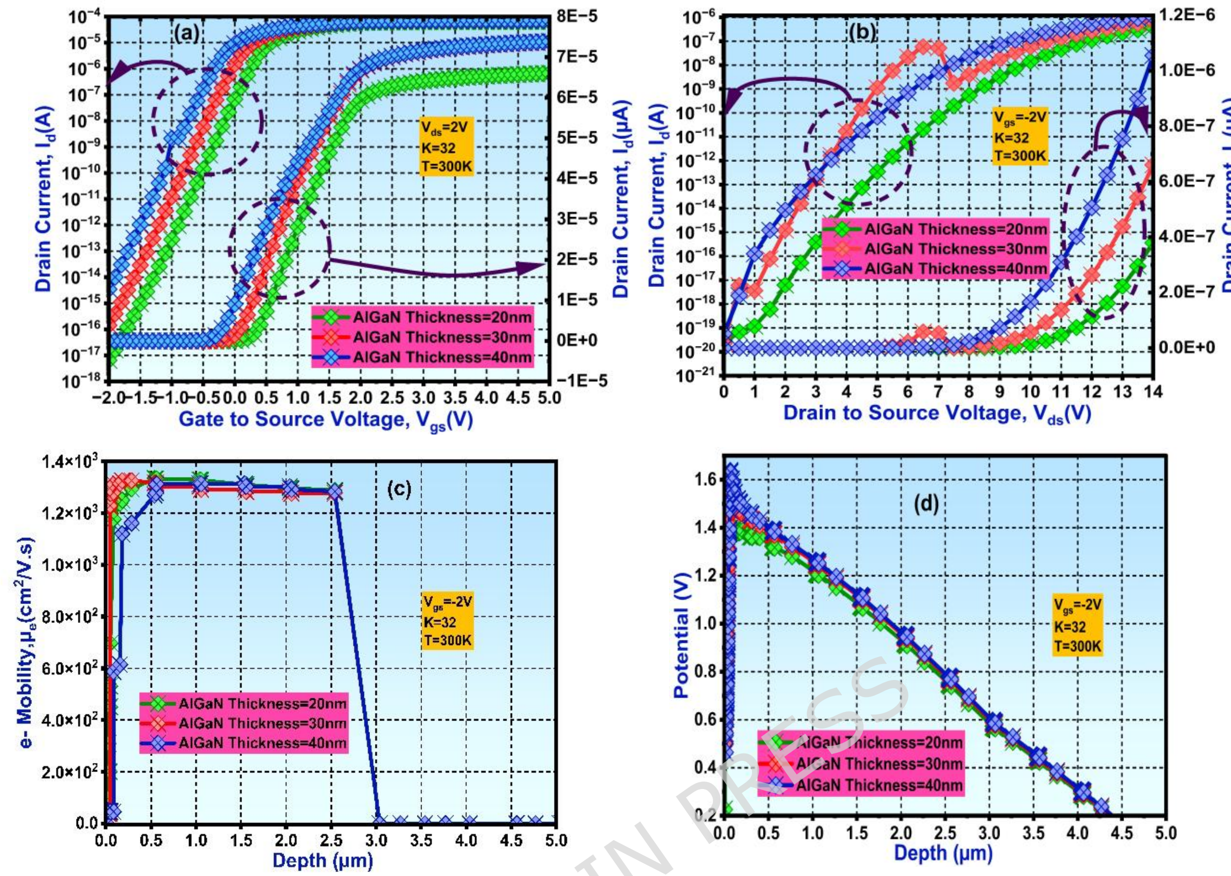

Figure.5 Electrical characteristics of the conventional AlGaN/GaN MOS-HEMT heterojunction for different AlGaN barrier thickness (20nm,30nm,40nm) (a) Transfer charcteristics (I_d-V_{gs}) (b) Output characteristics (I_d-V_{ds}) (c) electron mobility distibution along device depth (d) potential distribution along device depth.

The Al mole fraction is varied to enhance the electrical characteristics of the proposed AlGaN/GaN graded barrier MOS-HEMT heterojunction biosensor by optimizing the polarization-induced two-dimensional electron gas (2DEG) concentration at the AlGaN/GaN interface. The performance was evaluated using different Al compositions of 0.05,0.15,0.25 by fixing AlGaN thickness is 40nm of the dielectric constant K = 32 and the presence of neutral molecules with fixed charge density $q_f = 0$ in the conventional barrier MOS-HEMT heterojunction structure. Figure. 6(a) shows the transfer characteristics (I_d-V_{gs}) of the HEMT for different Al mole fractions in the AlGaN barrier layer. It can be noted from the results that the MOS-HEMT heterojunction structure with an Al mole fraction of 0.05 possesses better switching characteristics compared to other Al mole fraction MOS-HEMT heterojunction structures. The output characteristics (I_d-V_{ds}) shown in Figure. 6(b) further confirm that the 0.05 Al molefraction provides stable current conduction with reduced scatering effects. Overall, the device with 0.05 molefraction provides improves device performance by maintaing balanced polarization effects and stable carrier transport in the channel.

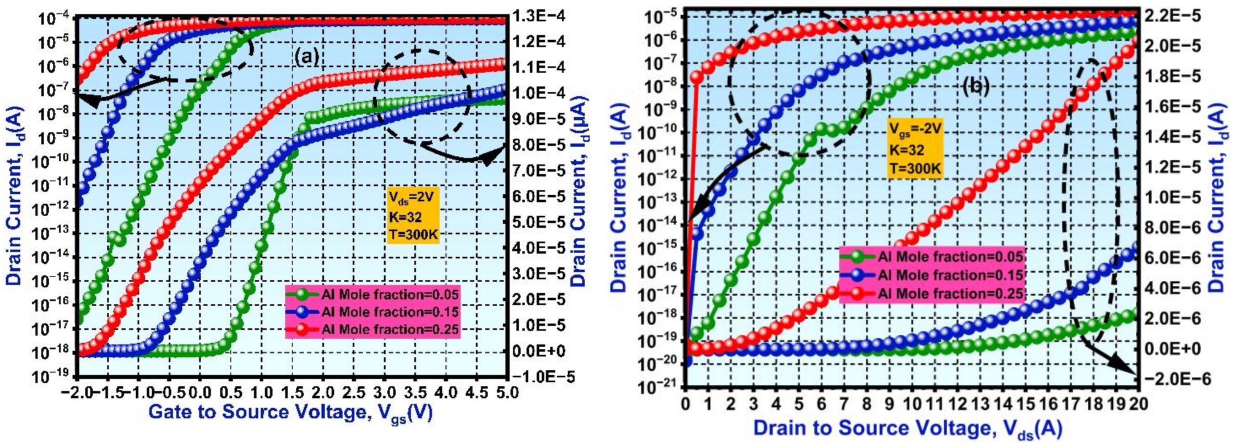

Figure. 6. Electrical characteristics of the conventional AlGaN/GaN MOS-HEMT heterojunction for different Al mole fraction (0.05,0.15,0.25) in the AlGaN barrier layer: (a) Transfer Charcteristics(I_d-V_{gs}) and(b) Output Characteristics(I_d-V_{ds})

B. Effect of Gate work function Engineering on device characteristics

The impact of gate work function engineering is studied to optimize its effect on the electrical characteristics of a typical AlGaN/GaN MOS-HEMT heterojunction structure with single metal gate (SMG), dual metal gate (DMG) and triple metal gate (TMG) structures with an aluminum mole fraction of 0.05. The gate work function has a significant impact on the channel potential and the carrier density in the two-dimensional electron gas (2DEG) at the AlGaN/GaN interface. Figure. 7(a) shows the output characteristics I_d-V_{ds} for the gate structures. It has been observed that the TMG structure exhibits a higher drain current compared to the single and dual metal gate structures.

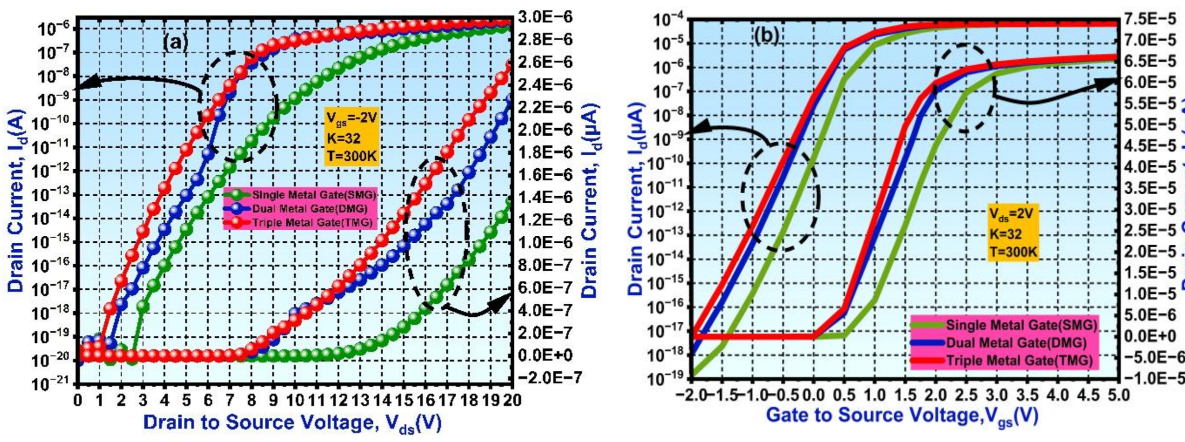

Figure. 7. Electrical characteristics of the conventional AlGaN/GaN MOS-HEMT heterojunction for single gate, dual gate and triple gate workfunctions: (a) Transfer Charcteristics(I_d-V_{gs}) and(b) Output Characteristics(I_d-V_{ds})

This enhancement occurs because the multiple gate workfunctions create a step like potential distribution along the channel, which improves carrier injection and redistributes the electric field, thereby lowering channel resistance. The transfer characteristics (I_d-V_{gs}) shown in Figure. 7(b), indicate that the TMG device has a higher switching capability when compared to the single and double metal gate devices. The use of multiple gate metals enhances electrostatic control over the channel and facilitates better carrier transport.

C. Evaluation of Barrier Engineering Effects in GaN-Based MOS-HEMT heterojunction Biosensors: Conventional vs. Graded AlGaN

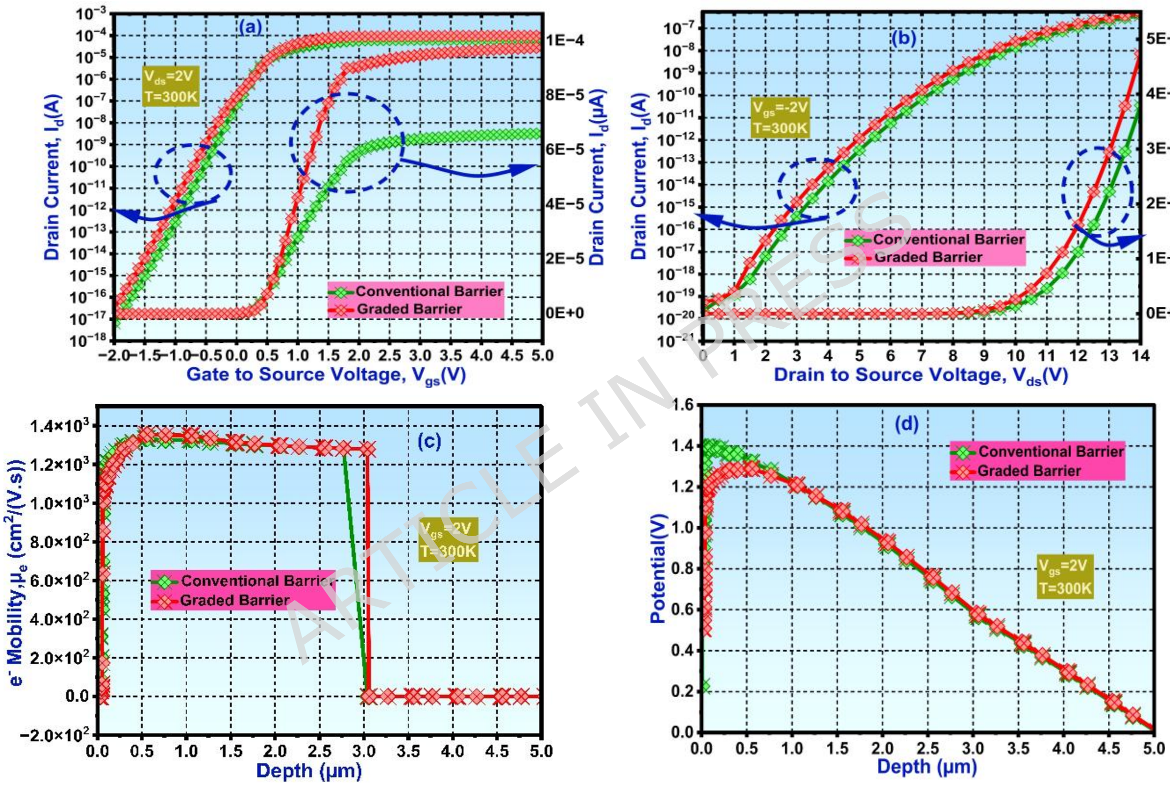

Figure. 8. Electrical characteristics of the conventional AlGaN/GaN MOS-HEMT heterojunction for Conventional vs. Graded AlGaN: (a) Transfer Charcteristics(I_d-V_{gs}) and(b) Output Characteristics(I_d-V_{ds}) (c) Electron mobility distibution along device depth (d) Potential distribution along device depth.

This section presents the comparative results obtained from the performance of the GaN MOS-HEMT heterojunction biosensor with graded and conventional AlGaN barrier structures. The thickness of the barrier is fixed at 40 nm for both structures. For the conventional structure, the Al composition is considered at 0.05 to ensure the stable formation of the two-dimensional electron gas (2DEG). In the graded AlGaN structure, the Al composition is varied linearly from 0 at the bottom to 0.05 at the top along the growth direction, changing the distribution of the polarization charges at the AlGaN/GaN interface. The detection of biomolecules is performed based on the differences in the dielectric properties of MCF-7 (cancerous) and MCF-10A (normal) cells influence the local electric field at the gate, thereby changing the drain current. The transfer characteristics, i.e., I_d-V_{gs}, are shown in Figure. 8(a), where it is observed that the graded AlGaN MOS-HEMT heterojunction shows higher drain current compared to the conventional AlGaN MOS-HEMT due to increased polarization effects that increases the concentration of 2DEG. Similarly, the output characteristics (I_d-V_{ds}) in Figure. 8(b) shows that the current levels are increased for the graded barrier device, and this is due to the uniform distribution of the electric field that reduces carrier scattering and channel resistances. Moreover, the electron mobility profile in the channel depth, as shown in Figure. 8(c), also shows an increased mobility for the graded barrier device due to reduced carrier scattering and better polarization characteristics. The vertical potential distribution is shown in Figure. 8(d) further confirms that the graded AlGaN barrier provides a uniform electric field in the channel region, thus enhancing device performance.

D. Electrostatic Analysis of Triple Metal Gate Work Function, Interface Trap Charges, and Polarization Effects

The variation of Triple Metal work function(TMG WKF) of proposed AlGaN/GaN graded barrier MOS-HEMT heterojunction-based biosensor is shown in Figure. (9). From Figure 9(a), it shows the variation in TMG work function of the electric field and the work function combination of 5.5/4.9/4.6 eV is high because it shows a high influence of the gate over the channel region. Figure. 9(b) shows an increase in TMG work function, the drain current sensitivity also increases. Thus, the drain current sensitivity obtained using the work function combination of 5.5/4.9/4.6 eV is maximum, while it gradually decreases with a decrease in work functions. Figure. 9(c) shows the threshold voltage (V_{th}) sensitivity, that increased work function values enhance the V_{th} sensitivity becauce of better channel charge modulation. The potential distribution along the channel, obtained from the contour potentials shown in Figure. 9(d), shows superior electrostatic behavior of the device. In other words, the optimized TMG work function leads to better channel control.

The effect of interface trap charge density on the sensitivities of I_d, SS and V_{th} is shown in Figure. 10(a). The sensitivities are maximized at negative values of interface traps, but a gradual decrease is seen in sensitivities as the interface trap charge increases to more positive values. Figure. 10(b) shows that there is a significant effect of polarization factor on device properties. The sensitivity of SS and V_{th} can be improved by increasing the polarization factor, which will further improve carrier confinement and electrostatic field control. The Triple Metal Gate(TMG) structure is engineered to ensure constant electrical connections in the sensing cavity, thus allowing for effective gate biasing and avoiding floating gate effects.

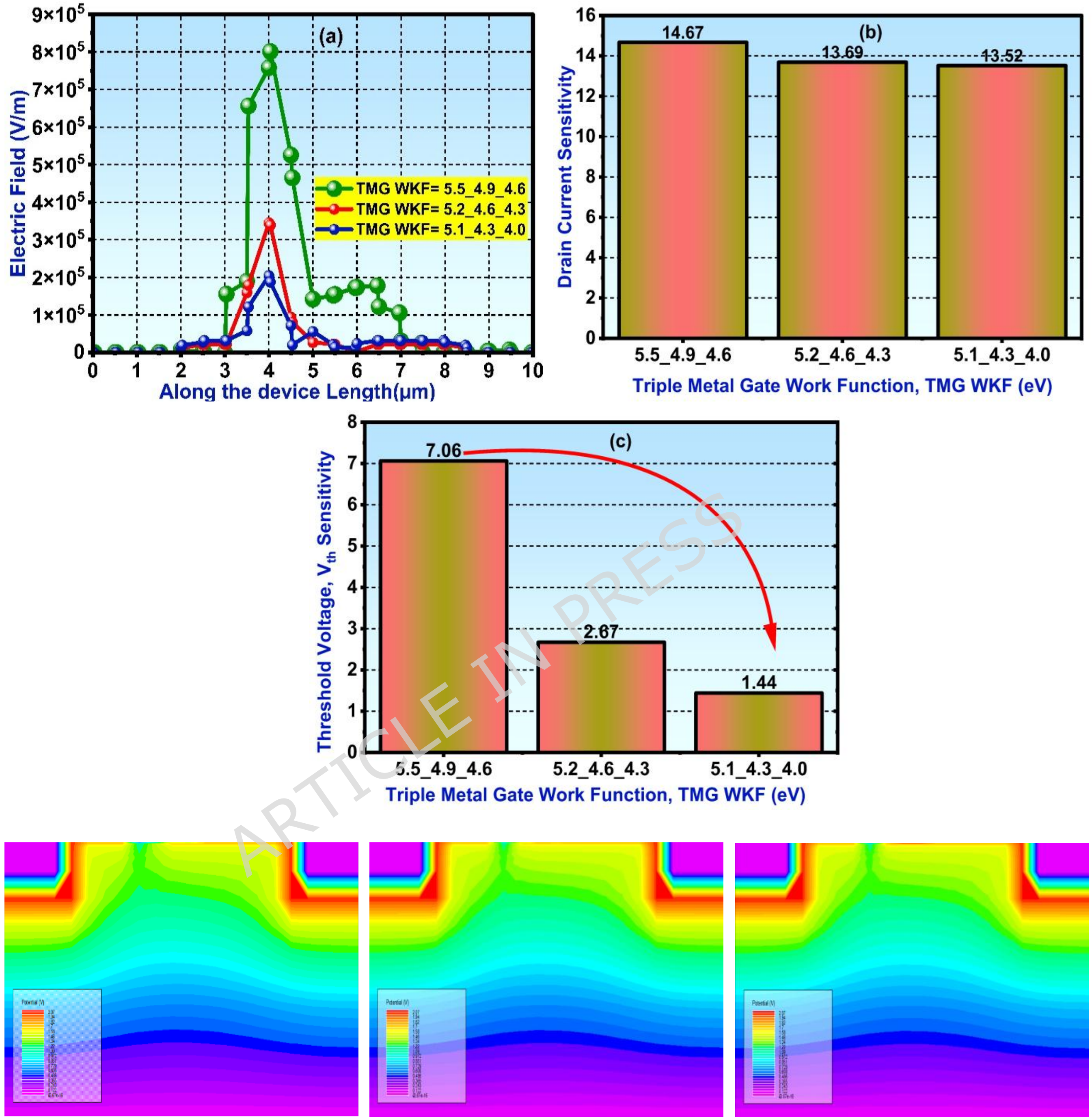

(d) (I)5.5_4.9_4.5 (II) 5.2_4.6_4.3 (III)5.2_4.3_4.0

Figure. 9. Effect of Triple Metal Gate (TMG) work function variation on the proposed graded barrier AlGaN/GaN MOS-HEMT: (a) Electric field distribution, (b) Drain current sensitivity, (c) Threshold voltage (V_{th})sensitivity, and (d) Potential contour distribution for different TMG work function combinations.

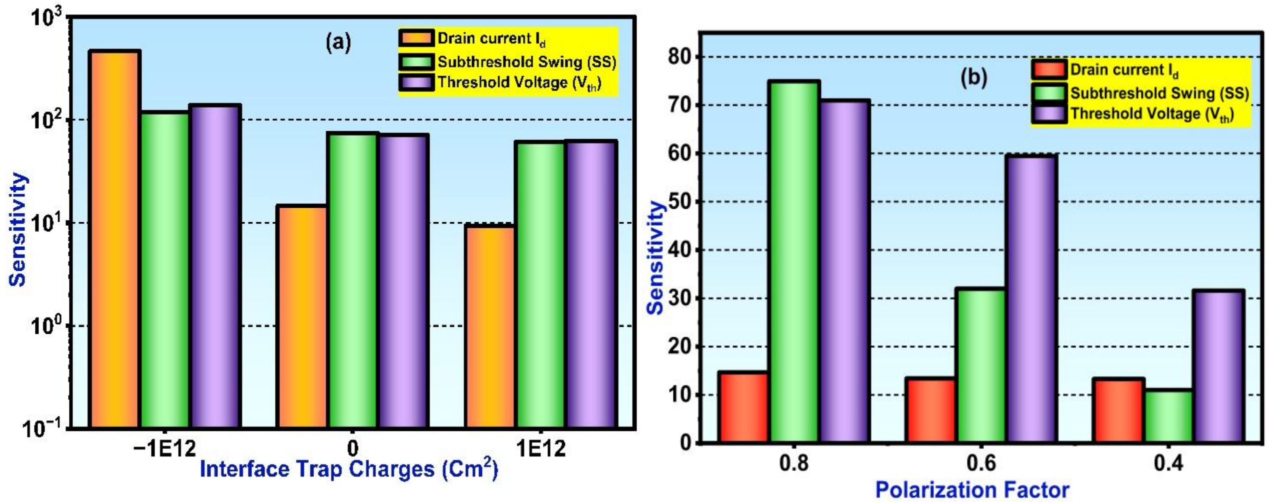

Figure. 10 Non-ideal effect analysis of the proposed graded barrier AlGaN/GaN HEMT: (a) Impact of interface charge density variation and (b) Polarization factor fluctuation on drain current sensitivity, subthreshold swing (SS), and threshold voltage sensitivity.

The C_{gs}-V_{gs} characteristics of the proposed AlGaN graded barrier MOS-HEMT at V_{ds}=2V, K=32 and T=300K. Figure. 11(a) shows the effect of conventional and graded AlGaN barrier structures on C-V characteristics. The graded barrier device exhibits higher Cgs values due to improved carrier distribution and reduced parasitic capacitance, which is beneficial for high-frequency operation. Figure. 11(b) shows the effect of dielectric materials such as SiO_2, Al_2O_3, HfO_2. Among them, the HfO_2-based device shows improved drain current characteristics and better electrostatic control because of its high dielectric constant. Figure. 11(c) shows the influence of HfO_2 dielectric thicknesses of 10 nm, 15 nm, and 20 nm. The 10 nm HfO_2 device provides the improved performance due to stronger gate-channel coupling and improved carrier modulation.

The gate-to-source capacitance was evaluated using the following analytical relation:[32]

$$C_{gs} = \frac{\mu_{o}(q\,W_{g\,\rho})^2}{I_{ds}} \left(\varphi_{gd}^{1/3} - \varphi_{gs}^{1/3}\right)\left(\frac{g_m}{I_{ds}} - 1\right) - \frac{q\,W_\rho}{E_T} V_{ds} - \frac{L_g\, g_m}{\mu_0 E_T} ----(1)$$

Where:

$$\varphi_{gs} = V_{gs} - V_{th} --- (2)$$

$$\varphi_{gd} = V_{gs} - V_{th} - V_{ds} ----(3)$$

and I_{ds} and g_m were extracted from the simulated transfer characteristics.

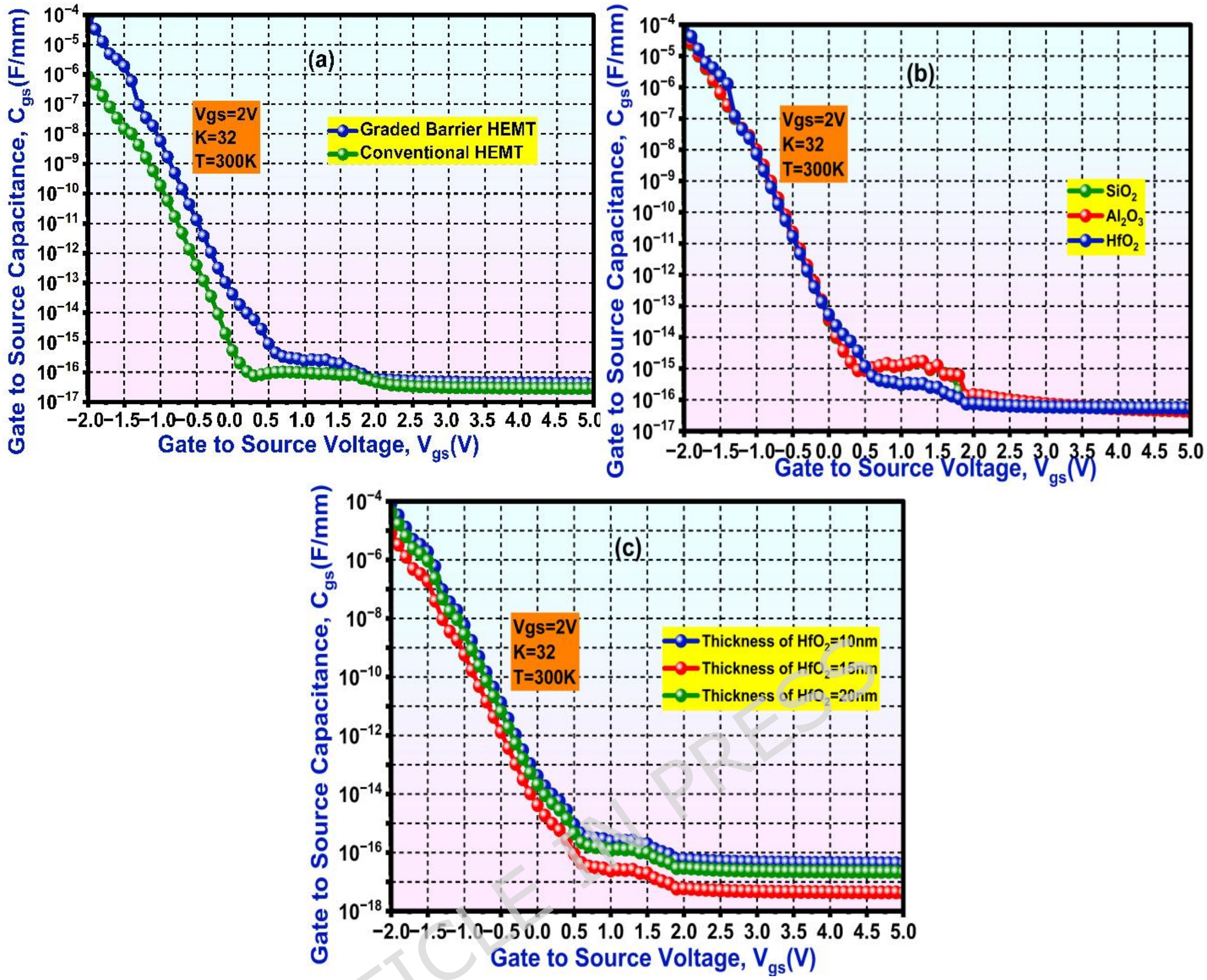

Figure: 11 C-V characteristics of proposed AlGaN graded barrier MOS-HEMT heterojunction (a) Conventional vs. Graded AlGaN (b) Dielectric Material variations (c) Dielectric Material thickness variations

E. Cavity Engineering

The cavity thickness and cavity length engineering is performed to optimize and improve the electrical performance and sensing capability of the proposed AlGaN/GaN graded barrier MOS-HEMT heterojunction biosensor by controlling the gate impact on the channel. The performances was evaluated using different cavity thickness (10nm,15nm 20nm) and cavity lengths (0.5µm,0.6µm,0.7µm) by fixing K=32 with zero charge density(q_f=0) and it is observed that the device exhibits improved performance as the cavity thickness decreases due to electron density in the 2DEG channel. The effect of cavity thickness(C_t) variation on transfer characteristics (I_d-V_{gs}) is shown in Figure. 12 (a). The variation in the thickness of the cavity affects the electric field in the region underneath the gate, thereby affecting the capacitance underneath the gate. As the thickness increases, the channel charge modulation is more pronounced, thereby affecting the subthreshold slope and the drain current. The effect of cavity length(C_l) variation on transfer characteristics (I_d-V_{gs}) is shown in Figure. 12(b). As the length of the cavity increases, the sensing region underneath the gate is enlarged, thereby affecting the channel potential by changing the capacitance underneath the gate. This causes a change in the carrier concentration in the channel, thereby changing the transfer characteristics. The cavity length and thickness play a important role in modulating the electrical characteristics of the AlGaN/GaN graded barrier MOS-HEMT heterojunction biosensor, enabling detection through changes in the I_d-V_{gs} responses.

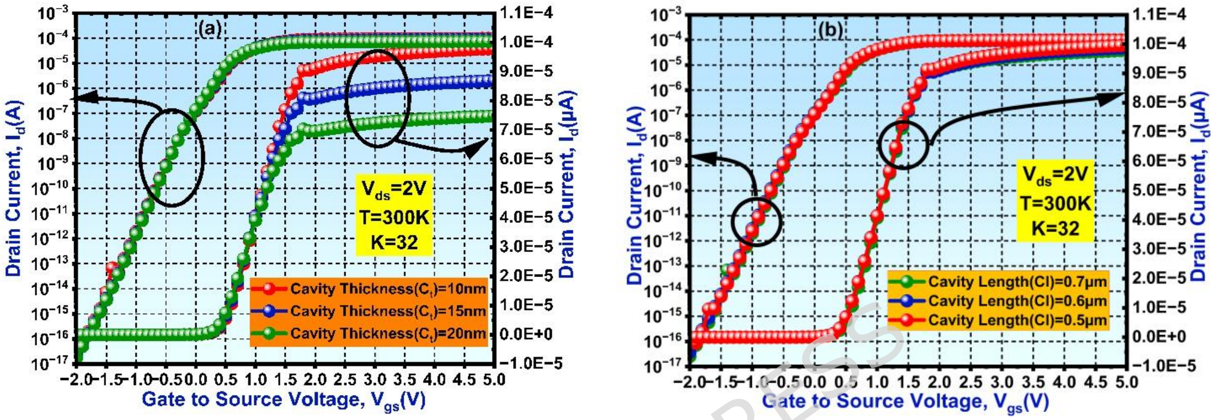

Figure. 12. Electrical characteristics of proposed AlGaN graded barrier MOS-HEMT heterojunction for cavity Engineering: (a) cavity thickness(C_t) and(b) cavity length(C_l)

F. Electrical Characteristics of the AlGaN/GaN graded barrier MOS-HEMT heterojunction device

The electrical characteristics of the AlGaN/GaN graded barrier MOS-HEMT heterojunction biosensor device are also analyzed based on the transfer characteristics (I_d-V_{gs}) and output characteristics (I_d-V_{ds}) of the device. In addition, the mobility of the electrons and the potential distributions are also considered to understand the device performance. Figure. 13(a) shows the transfer characteristics (I_d-V_{gs}) of the proposed biosensor device at K = 32. It is observed that the device drain current is increased with the gate voltage due to the formation of the high mobility 2DEG at the AlGaN/GaN interface. Figure. 13(b) shows the output characteristics (I_d-V_{ds}) of the proposed biosensor device, where the device drain current is increased with the increase in the drain voltage and then saturates, which is a typical HEMT device behavior. The graded barrier produces a smoother potential profile along the channel, which enhances carrier transport and minimizes scattering. Figure 13(c) and 13(d) shows contour plots of electron mobility and potential distributions of the proposed device, in which it is observed that the 2DEG channel of high mobility is achieved by incorporating the graded barrier layer, which enhances the overall performance of the device.

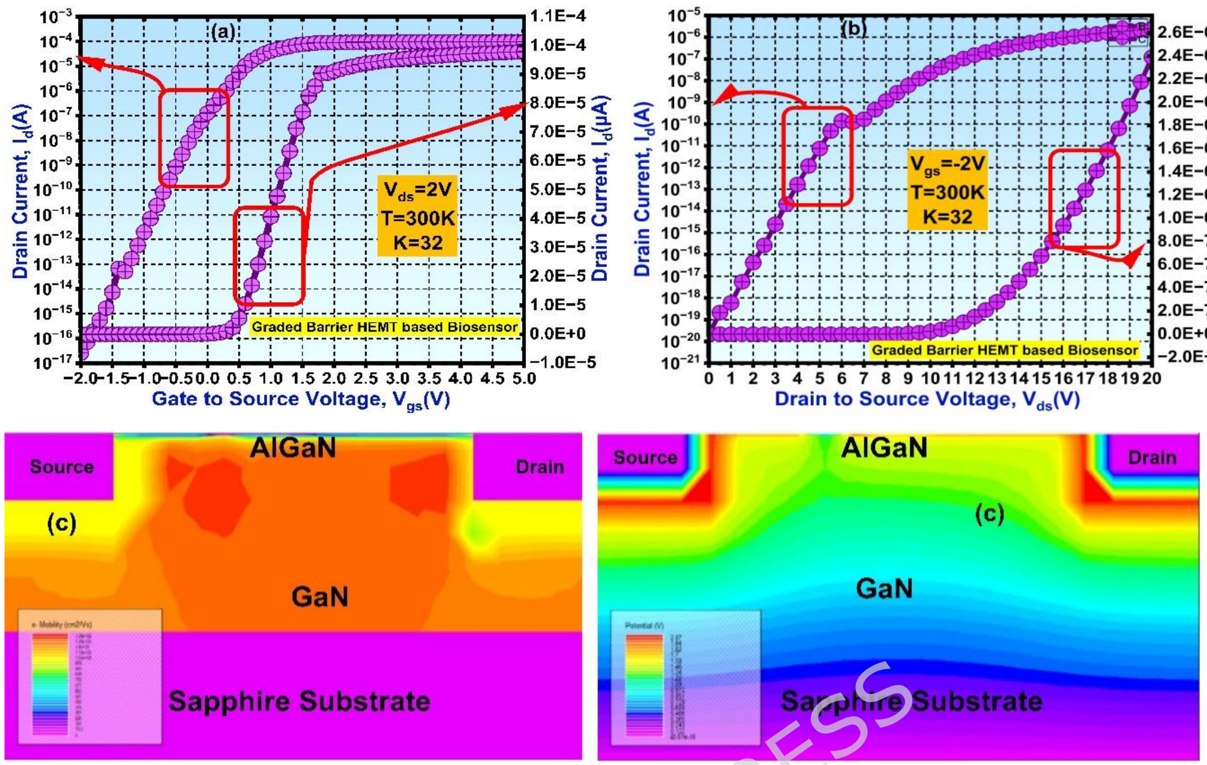

Figure. 13. Electrical characteristics of proposed AlGaN graded barrier MOS-HEMT heterojunction: (a) Transfer characterstics((I_d-V_{gs}) and(b) Output Characteristics(I_d-V_{ds}) (c) electron mobility contour plot (d) potential distribution contour plot.

G. Effect of Biomolecules

The effect of biomolecules on the proposed AlGaN/GaN graded barrier MOS-HEMT heterojunction biosensor device is essential for the detection of breast cancer. The transfer characteristics (I_d-V_{gs}) of the proposed AlGaN/GaN graded barrier MOS-HEMT heterojunction biosensor for various biomolecules with varying dielectric constants ranging from K = 1 (air) to K = 32 (T47D) by considering zero fixed charge density (q_f= 0) is shown in Figure. 14(a). The detection mechanism is based on the modulation of the 2DEG at the AlGaN/GaN interface due to polarization effects. As the biomolecules are placed in the cavity region of the proposed biosensor, the dielectric properties of the biomolecules influence the gate electric field and the channel potential, thereby affecting the channel charge density and drain current. The biomolecules with higher dielectric constants improve the channel conductivity by increasing the drain current and significantly changing the transfer characteristics. The differences in drain saturation current between different biomolecules facilitate the efficient recognition of these biomolecules based on dielectric constants, enhancing biosensors. The output characteristics (I_d-V_{ds}) of the proposed biosensor for various biomolecules with varying dielectric constants are shown in Figure. 14(b). The drain current increases for biomolecules with higher dielectric constants. Figure. 14(c) shows the transconductance characteristics (g_m-

V_{gs}),where g_m increases with the dielectric constant. Figure. 14(d) shows that g_m increases with the drain voltage, thereby increasing the conductivity in the channel. It is observed that the graded barrier MOS-HEMT heterojunction device can be used for Breast Cancer biomolecule sensing by observing the change in drain current and transconductance values.

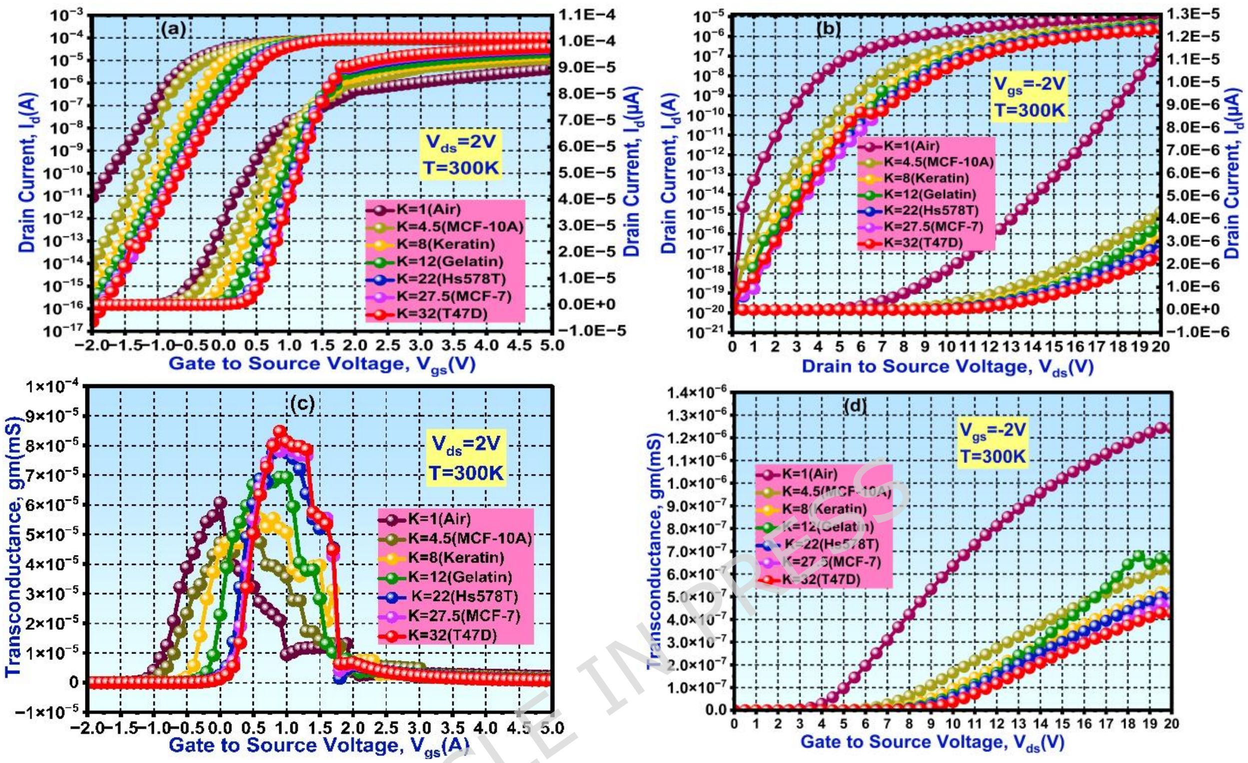

Figure. 14. Electrical characteristics of proposed AlGaN/GaN graded barrier MOS-HEMT heterojunction biosensor: (a) Transfer characterstics(I_d-V_{gs}) and (b) Output Characteristics(I_d-V_{ds}) (c) Transcondutance(g_m-V_{gs}) (d) Transcondutance (g_m-V_{ds}) .

TABLE-II
Electrical characteristics (I_{on}, I_{off}, I_{on}/I_{off} ratio, and threshold voltage) of the proposed AlGaN/GaN graded barrier MOS-HEMT heterojunction biosensor under varying dielectric constants (K)

Parameters	K=1	K=4.5	K=22	K=27.5	K=32
I_{on}	8.97x10^{-05}	9.36x10^{-05}	9.72x10^{-05}	9.76x10^{-05}	9.79x10^{-05}
I_{off}	8.53x10^{-12}	7.94x10^{-15}	4.46x10^{-17}	3.14x10^{-17}	2.54x10^{-17}
I_{on}/I_{off}	1.05x10^{+07}	1.18x10^{+10}	2.179x10^{+12}	3.11x10^{+12}	3.84x10^{+12}

H. Sensitivity Analysis

Sensitivity is also a major parameter for performance and is used to determine the ability of the biosensor to detect and determine the presence of different biomolecules. Sensitivity has been studied for different biomolecules such as neutral charge, negative charge and positive charge biomolecules. Sensitivity for the presence of biomolecules with neutral charge ($q_f = 0$) has been studied for different values of dielectric constants ranging from 4.5 to 32 for Breast Cancer biomolecules. Figure. 15(a) shows that increasing the dielectric constant (K) results in increasing the sensitivity gradually and reaches the maximum value of 0.147×10^2.

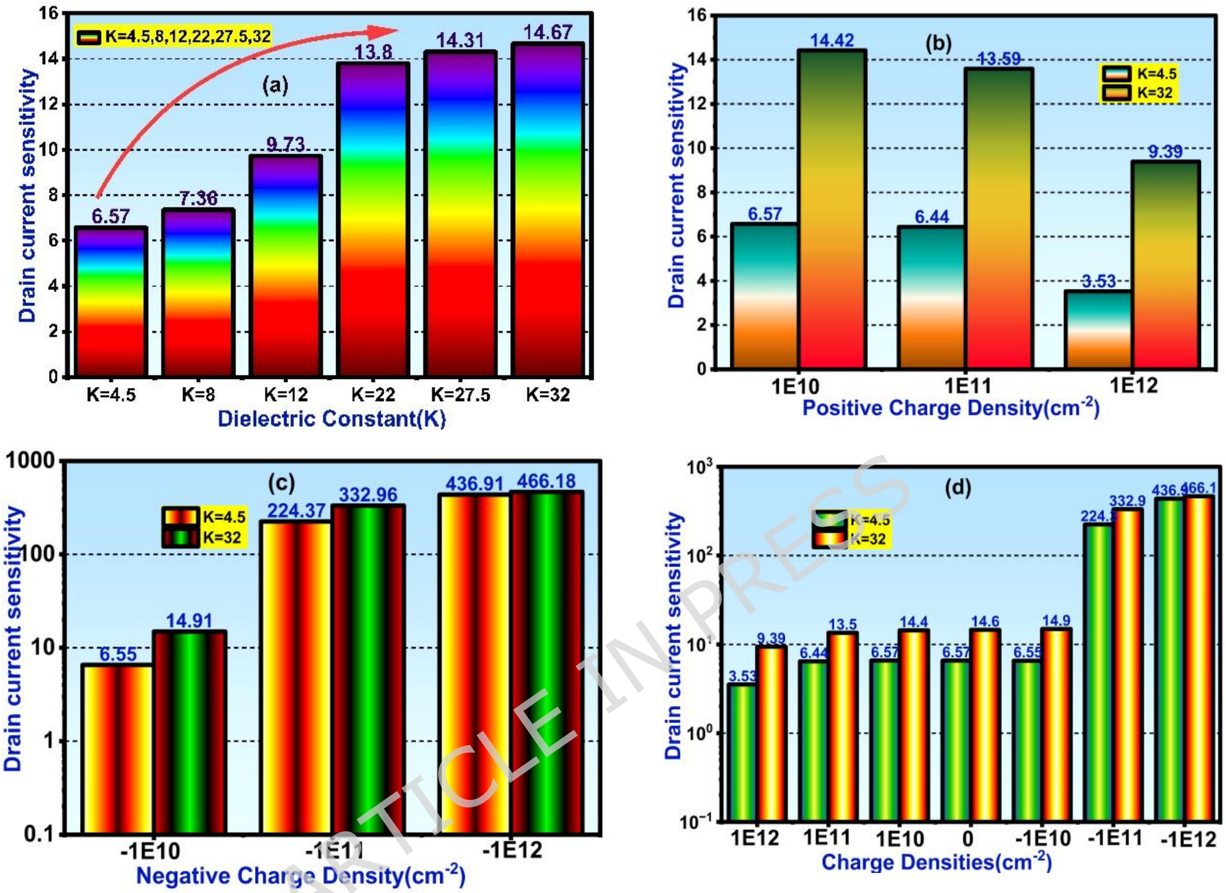

Figure. 15. Drain current(I_d) sensitivty analyses of proposed AlGaN/GaN graded barrier MOS-HEMT heterojunction biosensor: (a) Neutral charge density(q_f=0) (b) Positive charge density (q_f=+1E10, +1E11, +1E12) (c) Negaive charge density (q_f=-1E10, -1E11, -1E12) (d) All charge densities(q_f=+1E10, +1E11, +1E12,0, -1E10, -1E11, -1E12)

The sensitivity of positively charged biomolecules has been studied for charge densities ranging from (q_f= +1E10, +1E11, +1E12) for fixed dielectric constant(K) at K=32. Figure. 15(b) exhibits the maximum sensitivity of 0.142×10^2 confirming its ability to detect positively charged biomolecules. Same as negative charged biomolecules is evaluated for different charge density from (q_f= -1E10, -1E11, -1E12) for fixed dielectric constant(K) at K=32 and achieved a sensitivity of 0.466×10^3 as shown in Figure. 15(c). The overall variation of drain current sensitivity for both positive and negative charge densities is shown in Figure. 15(d). It is observed that negative charge density is significantly with much higher sensitivity compared to positive charge density. This indicates that the graded barrier MOS-HEMT heterojunction biosensor is highly sensitive to negatively charged biomolecules, which are generally associated with cancer-related species. The drain current (I_d) sensitivity and Transconductance (g_m) sensitivity is calculated using equation (4) and (5) respectively [34]. Figure. 16(a) shows that Transconductance (g_m) sensitivity increases as the value of the dielectric constant increase due to interaction between the gate and channel and increased modulation of carriers in the channel region. Similarly, Figure. 16(b) shows an improvement in sensitivity of I_{on}/I_{off} Ratio, that means the sensing mechanism can detect biomolecules effectively, exploiting their distinct dielectric properties. As Shown in Figure. 16(c) and Figure. 16(d), subthreshold swing (SS) sensitivity (6) and threshold voltage (V_{th}) sensitivity both increase with the dielectric constant.

$$Sensitivty, I_d = \frac{I_{d(bio)} - I_{d(air)}}{I_{d(air)}} \ x \ 100 ----(4)$$

$$Sensitivty, g_m = \left| \frac{g_{m(bio)} - g_{m(air)}}{g_{m(air)}} \ x \ 100 \right| --- (5)$$

$$Sensitivty, SS = \left| \frac{SS_{(bio)} - SS_{(air)}}{SS_{(air)}} \ x \ 100 \right| --- (6)$$

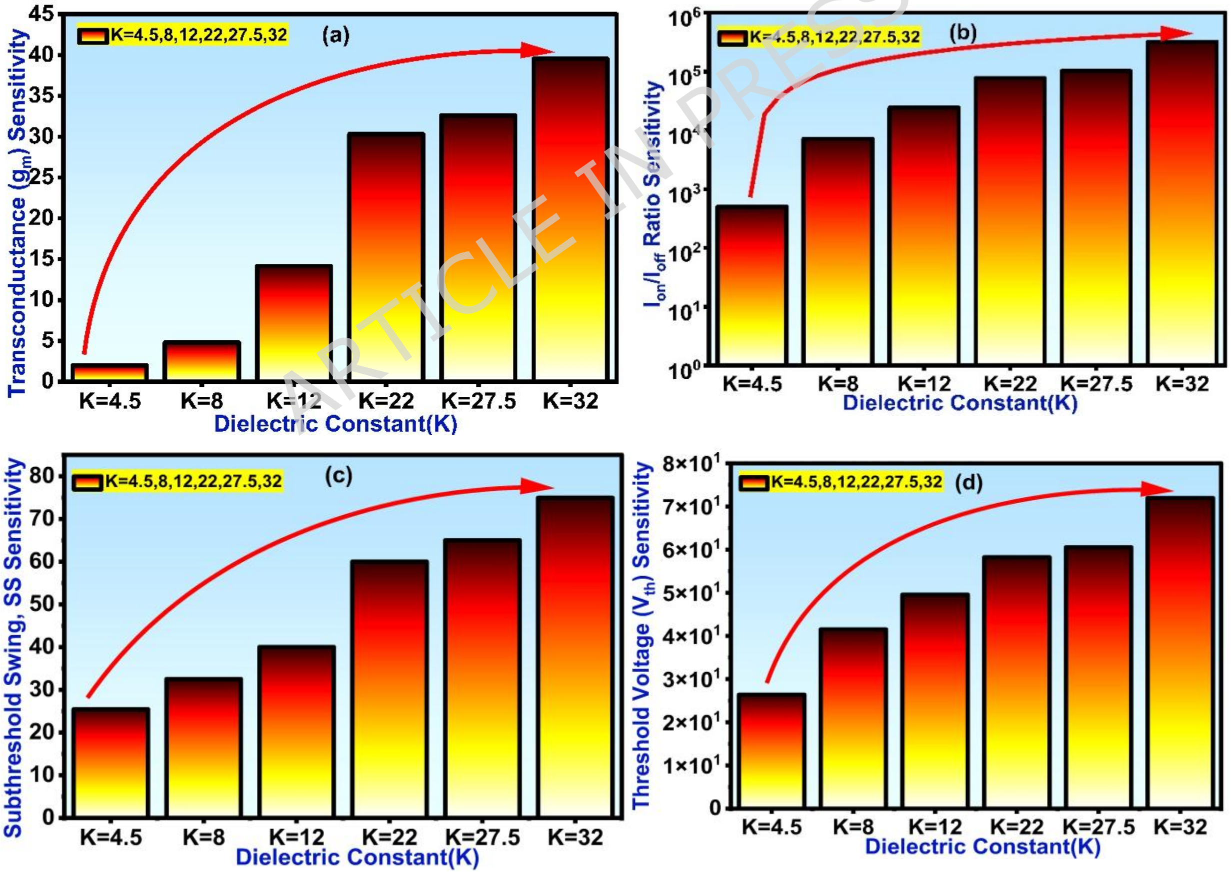

Figure 16. Sensitivity analysis of the proposed graded barrier AlGaN/GaN HEMT for different dielectric constants (K): (a) Transconductance (g_m), (b) I_{on}/I_{off} ratio sensitivity, (c) Subthreshold swing (SS) sensitivity, (d) Threshold voltage (V_{th}) sensitivity.

I. Performance analysis of the proposed device

To evaluate the sensing potential of the proposed AlGaN/GaN graded barrier MOS-HEMT heterojunction-based biosensor, parameters like response time, selectivity and LOD have been analyzed for various dielectric constants (K) of a different biomolecule.

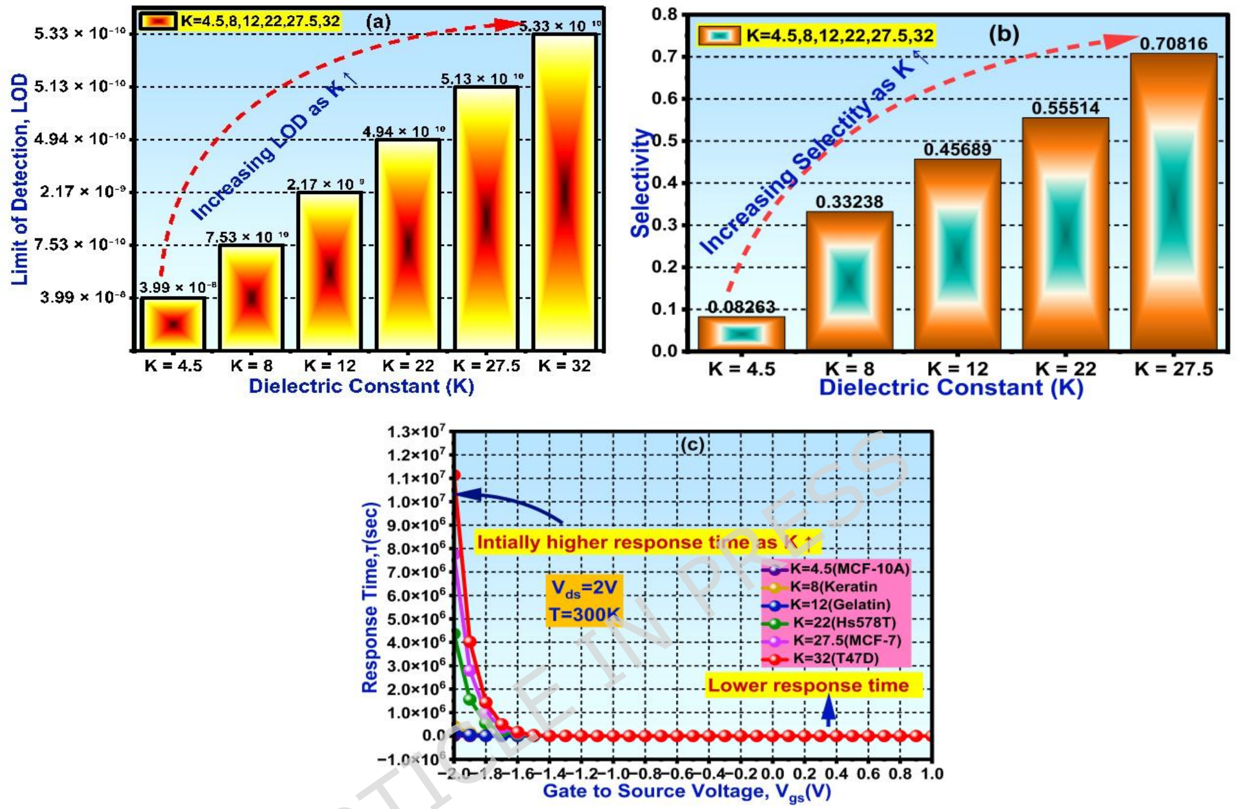

Figure. 17 Device performance characteristics of proposed AlGaN/GaN graded barrier MOS-HEMT heterojunction biosensor: (a) Limit of detection(LOD) (b) Selectivity (c) Response time(τ)

The limit of detection (LOD) is another important parameter, reflecting the sensing ability of the biosensor to detect different levels of biomolecule concentration. The improved sensing capability of the proposed MOS-HEMT heterojunction device is mainly due to the strong electrostatic interaction between the sensing cavity and channel. The limit of detection shown in Figure. 17(a) is calculated using equation (7). Figure. 17(b) shows the selectivity indicates that the proposed biosensor can distinguish between the target Breast Cancer biomolecules and other biomolecules having different dielectric constants. The selectivity increases smoothly with increasing dielectric constants. This is because of the stronger influence of the dielectric constants in the channel potential in the sensing area. The drain current (I_d) selectivity is calculated using equation (8) [33]. Figure. 17(c) shows the variation of response time with gate voltage (V_{gs}) for different dielectric constants (K) and observed that the response time is gradually lower for increasing gate voltage for different Dielectric constants (K), which shows that HEMT biosensors have a fast electrical response.

The response time is calculated using the equation (9), where Id is the drain current, K is dielectric constant value and permittivity ϵ_o =8.854x10^{-12} F/m.

$$LOD = \frac{3\ x\ \sigma}{S} - - - (7)$$

$$I_d Selectivity = \frac{I_d(target) - \ I_d(K = non - target)}{I_d(K = 32)} (8)$$

$$Response\ Time(\tau) = \frac{K\epsilon_o}{I_d} - - - (9)$$

J. Temperature Analysis

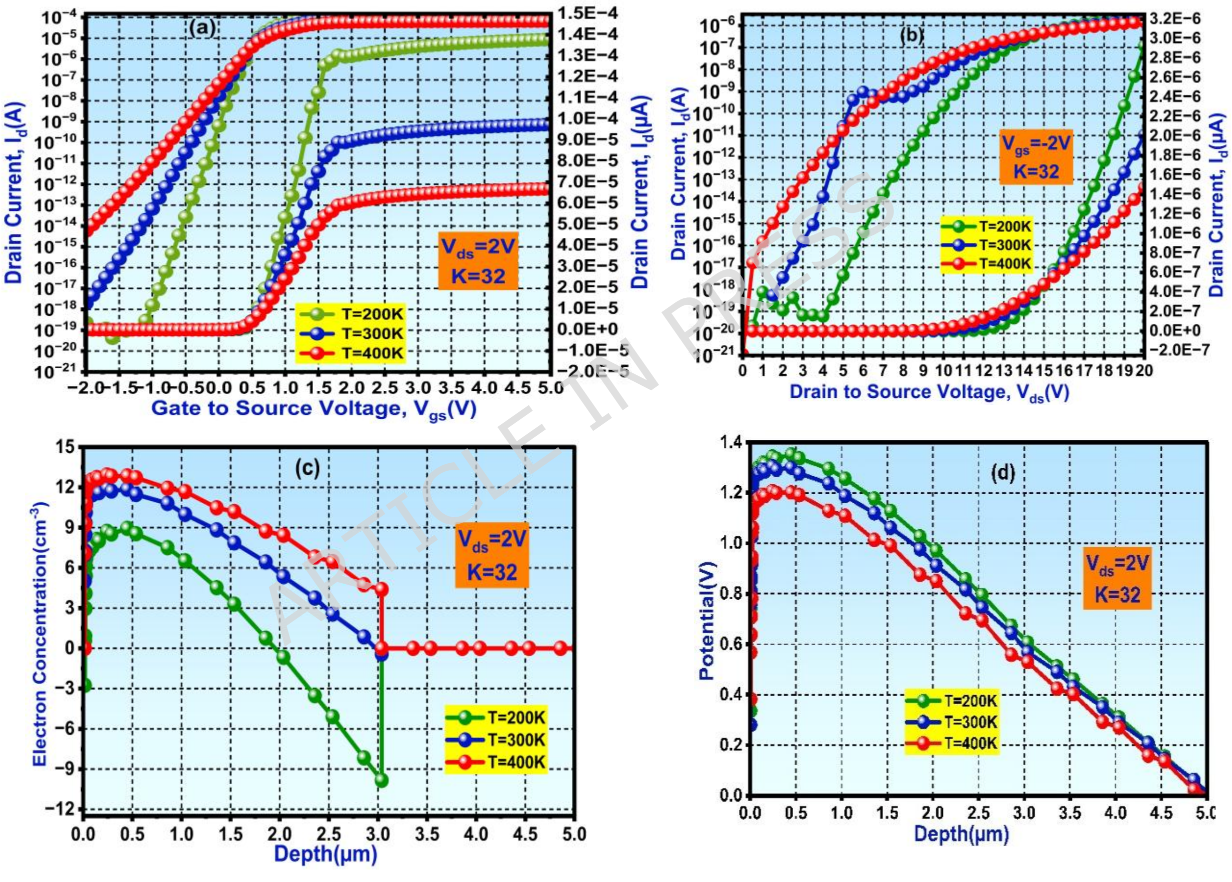

Figure. 18 Temperature analyses of proposed AlGaN/GaN graded barrier MOS-HEMT heterojunction biosensor: (a) Transfer characterstics((I_d-V_{gs}) and(b) Output Characteristics(I_d-V_{ds}) (c) electron mobility along depth(d) potential distribution along depth.

The temperature effect of proposed MOS-HEMT heterojunction biosensor was evaluated at different temperature 200K,300K and 400K by fixing K=32. The effect of temperature on the performance of the device is analyzed based on its electrical characteristics. As the temperature increases, there is a slight increase in the drain current due to the increased carrier generation and activity in the subthreshold region is shown in Figure. 18(a). At the same time, the variation in temperature causes carrier mobility, hence influencing the current. Figure. 18(b) shows the output characteristics at various temperatures and the drain current is observed to increase with the increase in drain voltage and saturate at higher voltage. As the temperature increases, there is a slight variation in the drain current due to increased carrier scattering. The electron concentration shown in Figure. 18(c) exhibits a peak at the AlGaN/GaN interface, indicating the formation of the two-dimensional electron gas (2DEG). As the temperature increases slightly, it influences the electron concentration. The potential distribution is obtained along the channel, showing a gradual decrease from the gate to the drain, indicating proper electric field distribution is shown in Figure. 18(d). The graded AlGaN barrier ensures a smooth change in potential, which is essential for maintaining a stable channel under varying temperature conditions.

K. Cavity Filling Factor

The cavity filling factor is used to describe how proposed device shows the percentage of the cavity filled with biomolecules, which affects the performance of proposed AlGaN/GaN graded barrier MOS-HEMT heterojunction biosensor. We have also studied the cavity filling factor for 25%-100% filling with biomolecules by fixing the value of K at 32 as shown in Figure. 19(a). The drain current is gradually increasing for higher percentages of filling. This is because the gate coupling is increasing and the 2DEG carrier density is also increasing at the AlGaN/GaN interface. Figure. 19(b) is the output characteristics (I_d-V_{ds}), and it is observed that the device with higher percentages of cavity filled has higher drain current for the entire range of drain voltage. The Cavity Filling Factor is calculated using the equation(10).

$$\gamma bio = \frac{Thickness\ of\ the\ cavity\ filled}{Total\ Thickness\ of\ the\ cavity}\ x\ 100 - - - (10)$$

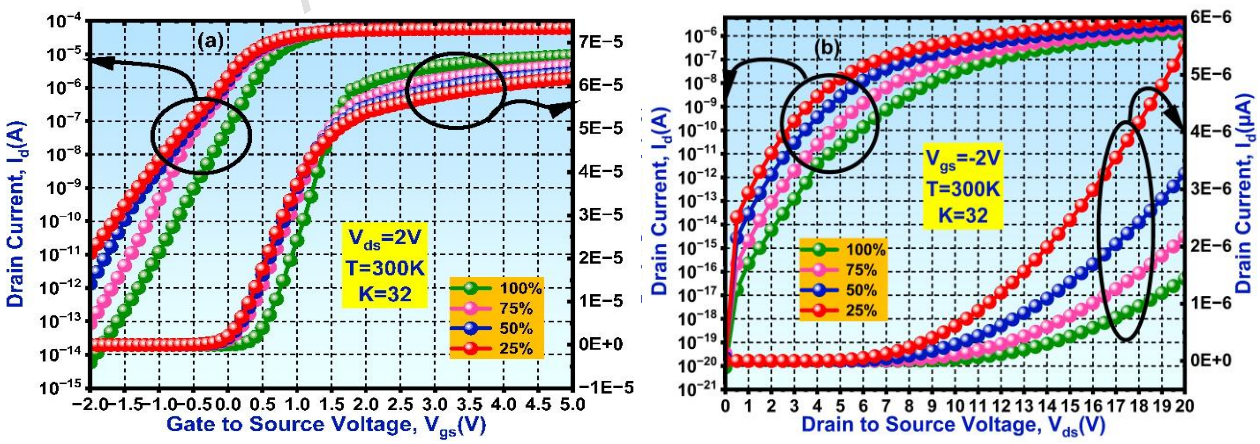

Figure. 19 Cavity filling factor of proposed AlGaN/GaN graded barrier MOS-HEMT heterojunction biosensor: (a) Transfer characterstics((I_d-V_{gs}) and(b) Output Characteristics (I_d-V_{ds})

Table -III shows the steric hindrance effect due to the position and concentration of biomolecules inside the cavity of the suggested device. The shaded region indicates the percentage of biomolecule occupancy and their location inside the cavity, both of which are critical factors for the electrical characteristics of the sensor. This analysis has been carried out for biomolecules with dielectric constants K=4.5 to K=32, considering both cases of biomolecule positioning, i.e., center/inner filling (Case 1) and edge-based filling (Case 2), while the occupancy level is fixed at 30%. The results clearly show that edge-based filling (Case 2) offers better I_{on}/I_{off} ratio sensitivity and V_{th} sensitivity compared to the center/inner filling (Case 1) configuration. This is due to the better dielectric effect of biomolecules near the junction of the source and channel, where the electric field is higher compared to other junctions in HEMT devices. However, excessive biomolecule accumulation near the boundaries of the cavity for 30% edge-based filling may lead to steric hindrance, thus slightly reducing the sensitivity of the sensor compared to the center-based configuration. The I_{on}/I_{off} ratio sensitivity and V_{th} sensitivity is calculated using equation (11) and (12), respectively.

$$Sensitivty, I_{on}/I_{off} = \left| \frac{I_{on}/I_{off\,(bio)} - I_{on}/I_{off\,(air)}}{I_{on}/I_{off\,(air)}} \, x\ 100 \right| - (11)$$

$$Sensitivty, V_{th} = \left| \frac{V_{th(bio)} - V_{th(air)}}{V_{th(air)}} \, x\ 100 \right| - - - (12)$$

L. Signal to Noise Ratio

To evaluate the sensing potential of the proposed AlGaN/GaN graded barrier MOS-HEMT heterojunction-based biosensor, parameters SNR have been analyzed for various dielectric constants (K) of a different biomolecule. Figure. 20 shows the variation of signal-to-noise ratio (SNR) with different dielectric constants of the Breast Cancer biomolecules. As the dielectric constant of the biomolecules increases from K=4.5 to K=32, it is observed that the biosensor is more sensitive to detecting the presence of the

TABLE-III

Effect of biomolecule coverage and spatial arrangement on the sensing performance of the proposed biosensor

No. of Cases	Green Shaded Area represents the habitation of Biomolecules										Cavity's occupied Area	I_d-V_{gs} I_{on}/I_{off} Ratio Sensitivity		I_d-V_{gs} V_{th} Sensitivity	
												MCF-10A (K=4.5)	T47D (K=32)	MCF-10A (K=4.5)	T47D (K=32)
1			■					■	■		30%	$6.10x10^{01}$	$1.53x10^{02}$	$6.41x10^{00}$	$1.31x10^{01}$
2	■								■	■	30%	$7.03x10^{01}$	$2.34x10^{02}$	$6.98x10^{00}$	$1.52x10^{01}$
3		■	■			■		■			40%	$9.53x10^{01}$	$4.86x10^{02}$	$8.61\ x10^{00}$	$1.74\ x10^{01}$
4		■	■		■				■	■	50%	$1.67x\ x10^{02}$	$1.64\ x10^{03}$	$1.08\ x10^{01}$	$2.20\ x10^{01}$
5	■	■		■	■		■	■			60%	$4.10\ x10^{02}$	$5.11\ x10^{03}$	$1.31\ x10^{01}$	$2.66\ x10^{01}$
6		■	■	■			■	■	■	■	70%	$9.43\ x10^{02}$	$1.55\ x10^{04}$	$1.53\ x10^{01}$	$3.16\ x10^{01}$
7		■	■	■		■	■	■	■	■	80%	$2.04\ x10^{03}$	$4.65\ x10^{04}$	$1.76\ x10^{01}$	$4.01\ x10^{01}$
8		■	■	■	■	■	■	■	■	■	90%	$4.31\ x10^{03}$	$1.40x\ x10^{05}$	$2.01\ x10^{01}$	$6.79\ x10^{01}$

biomolecules since biomolecules with higher dielectric constants create stronger coupling between the gate electric field and the channel current, resulting in stronger modulation of the two-dimensional electron gas (2DEG) current signal compared to noise current. The signal-to-noise ratio (SNR) is determined using equation (13).

$$SNR = \frac{\Delta I}{\sigma} - - - (13)$$

where, ΔI is change in current due to the presence of the target biomolecule, σ is standard deviation of the current in the air.

TABLE-IV
Comparative evaluation of the proposed AlGaN/GaN graded barrier MOS-HEMT biosensor with previously reported HEMT-based biosensors

Devices	Sensitivity	Subthreshold Swing, SS (mV/dec)	I_d-V_{gs} I_{on}/I_{off} Ratio	I_d-V_{gs} V_{th} Sensitivity	I_d-V_{gs} I_{on}/I_{off} Ratio Sensitivity	Operating Voltage (V_{ds})
This Work – Negative charge	4.66×10^2	58	9.30×10^{14}	3.46×10^2	7.89×10^5	-2.5
This Work – Neutral	1.47×10^1	60	3.85×10^{12}	8.92×10^1	1.40×10^5	
This Work – Positive charge	0.939×10^1	183	8.94	4.56	16.860	
AlN/ß-Ga_2O_3 HEMT [13]	3.6×10^1	80	2.75×10^3	2.12×10^1	1.00×10^2	-6
AlGaN/GaN HEMT [10]	3.75×10^1	-	2.5×10^3	0.7	40	-1.5
Boron doped HEMT [14]	0.25	-	4.1×10^5	0.245	5	-3

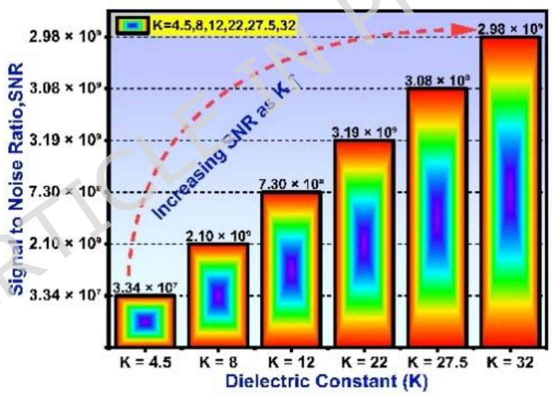

Figure. 20 Device performance characteristics of proposed AlGaN graded barrier MOS-HEMT heterojunction: Signal to Noise Ratio(SNR)

M. Performance comparison with existing HEMT biosensors

A comparison with existing HEMT devices is essential for validating the performance of the proposed biosensor. Sensitivity, subthreshold swing, I_{on}/I_{off} ratio and voltage operation of the AlGaN/GaN graded barrier MOS-HEMT heterojunction device highlight its enhanced electrical and sensing performance. The subthreshold swing(SS) of the device is calculated using equation (14) [3].

$$Subthresold\ Swing(SS) = \frac{\delta V_{gs}}{\delta log\ I_{ds}} - - - (14)$$

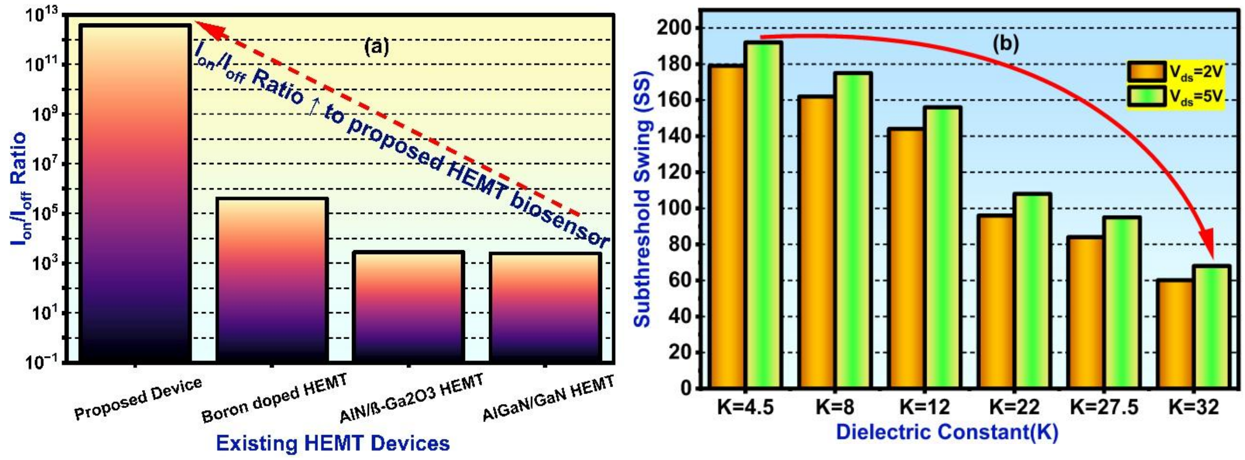

Figure. 21 (a) Comparsion of proposed AlGaN graded barrier MOS-HEMT heterojunction with existing devices (b) Subthreshold swing (SS) variation of the proposed graded barrier AlGaN/GaN HEMT for different dielectric constants under V_{ds}=2V and V_{ds}=5V conditions.

Table IV shows a comparison between the proposed AlGaN/GaN graded barrier MOS-HEMT heterojunction biosensor and earlier reported HEMT-based biosensors. The main parameters considered in this comparison are sensitivity, sub-threshold swing (SS), the I_{on}/I_{off} ratio of 3.85×10^{12} and the operation voltage of -2.5V. The proposed biosensor has a sensitivity of 1.47×10^1, a SS of 60 mV/decade and an I_{on}/I_{off} ratio indicating strong control of the gate signal and significant modulation of the 2DEG channel at the AlGaN/GaN interface. Compared with earlier AlN/β-Ga_2O_3 and conventional AlGaN/GaN HEMT structures, the proposed biosensor has a high I_{on}/I_{off} and better switching characteristics due to strong carrier confinement within the graded AlGaN barrier is shown in Figure. 21(a). Figure. 21(b) shows the relation between SS and the dielectric constant for V_{ds}=2V and V_{ds}=5V. It can be observed that the decrease in SS value occurs gradually with the increasing in dielectric constant(K), because of better electrostatic gate-channel coupling and better channel control. In both cases of the drain voltage condition, the minimum SS value is obtained when the dielectric constant is K=32. Though there is an increase in the SS value at V_{ds}=5V compared to V_{ds}=2V because of increased drain electric field effect, the proposed biosensor shows desirable characteristics even in the higher case of dielectric constant.

IV. Conclusion

In this article, we have proposed an AlGaN graded barrier MOS-HEMT heterojunction biosensor for Breast Cancer biomolecule detection. The purpose of graded AlGaN barrier stacked over the GaN layer enhance polarization-induced charge and increase the two-dimensional electron gas(2DEG) density at interface. The device is also simulated using Silvaco ATLAS TCAD, showing enhanced electrostatic performance with parameters of V_{th} sensitivity of 8.97 $\times 10^1$, I_{on}/I_{off} ratio sensitivity of 3.67×10^5. The proposed biosensor is effective in detecting Breast Cancer biomolecules with sensitivities of 0.147×10^2 for neutral, 0.9×10^1 for positive, and $4.66x10^2$ for negative biomolecules. The analysis of steric hindrance and cavity filling factor also showed that increased occupancy of biomolecules and edge-based filling increase the performance of the proposed biosensor due to increased interaction of the electric field with the channel. In addition, temperature analysis was performed that the proposed biosensor is stable under different temperature variations and making it suitable for biosensing applications. Future work may focus on improving the sensitivity and selectivity of the MOS-HEMT biosensor by optimizing the barrier layer and gate structure. In addition, experimental validation and integration with advanced sensing cavities can further enhance its performance for practical biomedical sensing applications.

Acknowledgements: The authors thank to the department of Electronics and Communications Engineering, Koneru Lakshmaiah Education Foundation (Deemed to be University), Green Fields, Vaddeswaram, Guntur, Andhra Pradesh, for providing the necessary Computational Tools.

Funding: No Funding Received

Authors' Contribution: Dr.Srinivasa Rao Karumuri, Rudra Lakshmi Prasanna: Writing- Original draft preparation, Formal Analysis, Investigation, Simulation, Data Curation. Dr. V B Sreenivasulu & Dr.Girija Sravani Kondavitee: Supervision, Resources. All authors read and approved the final manuscript.

Data Availability: The authors confirm that all data are included within the manuscript.

Declarations: Ethics Approval The manuscript in part or full has not been submitted or published anywhere. The manuscript will not be submitted elsewhere until the editorial process is completed.

Consent to Participate: Not applicable.

Consent for Publication: Not applicable.

Research Involving Human Participants and / or Animals: Not applicable.

Informed Consent: Not applicable.

Competing Interests: The authors have no conflicts of interest to declare that are relevant to the content of this article.

Authors' Information:

Dr.Srinivasa Rao Karumuri -- Working as Professor in the Department of Electronics and Communication Engineering, Koneru Lakshmaiah Education Foundation (Deemed to be University).

Rudra Lakshmi Prasanna – Working as Research Scholars in the Department of Electronics and Communication Engineering, Koneru Lakshmaiah Education Foundation (Deemed to be University).

VB Sreenivasulu– Assistant Professor in Department of Electronics and Communication Engineering, Manipal Institute of Technology, Bengaluru.

Dr.Girija Sravani Kondavitee -- Working as a Associate Professor in the Department of Electronics and Communication Engineering, Koneru Lakshmaiah Education Foundation (Deemed to be University).

Disclosure of Potential Conflicts of Interest: The authors have no relevant financial or non-financial interests to disclose.

References

[1] Kim, J. et al. "Global patterns and trends in breast cancer incidence and mortality across 185 countries," *Nat Med 31*, 2025. doi:10.1038/s41591-025-03502-3.

[2] R. Anil Kumar, et al. "A Novel T-Shape Channel With an Inverted-T Nano-Cavity Label-Free Detection Using Si:HfO2 Ferroelectric DGDM-JLTFET as a Biosensor—A Simulation Study," *IEEE Sensors Journal*, 2024, doi: 10.1109/JSEN.2024.3459100.

[3] Prasanna, R.L., et al. "Design and analysis of doping-less dielectric modulated tunnel FET biosensor for label free detection of breast cancer biomolecules," *Microsystem Technology 31*, 2025, doi:10.1007/s00542-025-05938-6.

[4] S. R. Karumuri, et al. "Analysis of an Electrically Doped Dielectric Modulated TFET Biosensor Design for Label Free Detection of Breast Cancer Cells," *IEEE Sensors Journal*, 2025, doi: 10.1109/JSEN.2025.3648039.

[5] R. Anil Kumar, et al., "A Novel T-Shape Channel With an Inverted-T Nano-Cavity Label-Free Detection Using Si:HfO2 Ferroelectric DGDM-JLTFET as a Biosensor—A Simulation Study," *IEEE Sensors Journal*, 2024, doi: 10.1109/JSEN.2024.3459100.

[6] G. S. Kondavitee, et al., "Design and Performance Analysis of N+ Pocket-Doped Vertical DMDGDP TFET with T-Shape channel for Sensitivity Improvement---As a Biosensor," *IEEE Sensors Journal*, doi: 10.1109/JSEN.2024.3476693.

[7] B. M. Lowe, et al. "Field-effect sensors—From pH sensing to biosensing: Sensitivity enhancement using streptavidin–biotin as a model system," *Analyst*, 2017, doi: 10.1039/C7AN00455A.

[8] S. J. Pearton, et al. "Functionalized GaN-based transistors for biosensing," State of the Art in Biosensors: Environmental and Medical Applications, 2013, doi: 10.5772/50351.

[9] Y. Liu et al. "Enhancement of Sensing Performance of GaN-Based MOS-HEMT Biosensors by Graded AlGaN Barrier," *IEEE Sensors Journal*, 2024, doi: 10.1109/JSEN.2024.3409708.

[10] R. Poonia, et al. "Performance Assessment of AlGaN/GaN HEMT for Human Serum Albumin Detection Using Charge Deduction Methodology," *IEEE Sensors Journal*, 2024, doi: 10.1109/JSEN.2024.3385496.

[11] R. R. Thakur, et al. "First Demonstration of GaN HEMT-Based Handheld System for Noninvasive Detection of Traumatic Brain Injury Using Saliva," *IEEE Sensors Journal*, 2024, doi: 10.1109/JSEN.2023.3334364.

[12] S. Mishra, et al. "AlGaN/GaN HEMT Based Biosensor for Detection of the HER2 Antigen Spiked in Human Serum," *IEEE Transactions on Electron Devices*, 2022, doi: 10.1109/TED.2022.3184658.

[13] A. Tomar, et al. "AlN/β–Ga_2O_3 HEMT-Based Biosensor for Sensitive Detection of Cardiac Troponin I via Charge Deduction Methodology," *IEEE Sensors Journal*, 2025, doi: 10.1109/JSEN.2025.3606461.

[14] Hemalatha, R.G., et al. "Design and Simulation of advanced boron-doped GaN cap layer on AlGaN/GaN MOSHEMTs for enhanced label-free biosensing applications," *Biomed Microdevices 27*, 2025, doi:10.1007/s10544-025-00746-1

[15] Fauzi, N., et al. " AuNis modified AlGaN/GaN HEMT biosensor for reliable detection of small Rho GTPases in Jurkat T cell lysate," *Sci Rep 15*, 2025, doi:10.1038/s41598-025-18072-0.

[16] N. Chaturvedi et al. "GaN HEMT based biosensor for the detection of breast cancer marker (C-erbB2)," *Semicond.Sci.Technol.*,2021, doi:10.1088/1361-6641/abe83e.

[17] N. Sharma et al., "High-resolution AlGaN/GaNHEMT-based electrochemical sensor for biomedical applications," *IEEE Trans. Electron Devices*, 2020, doi: 10.1109/TED.2019.2949821.

[18] S.Mishra, et al. "Detection of heavy metal ions using meander gated 492 GaN HEMT sensor," *Sens. Actuators A, Phys.*, 2021, doi: 10.1016/J.SNA.2021.113119.

[19] N.Chaturvedi, et al. "AlGaN/GaN HEMT based sensor and system for polar liquid detection, *Sens.ActuatorsA,Phys.*, 2020, doi:10.1016/j.sna.2019.111799.

[20] S.Mishra, et al. "Simulation and machine learning modelling based comparative study of InAlGaN and AlGaN high electron mobility transistors for the detection of HER-2," *Anal. Methods*, 2021, doi:10.1039/D1AY00707F. 501.

[21] P.Kachhawa et al. "Antigen-antibody interaction-based GaN HEMT 502 biosensor for C3G detection," *IEEE Sensors J.*, 2022, doi:10.1109/JSEN.2022.3150027.

[22] Shaveta, Ahmed, et al. "Rapid detection of biomolecules in a dielectric modulated GaN MOSHEMT," *J Mater Sci: Mater Electron 31*, 2020, doi:10.1007/s10854-020-04216-7.

[23] L. Arivazhagan, et al. "Applicability of double Channel Technique in AlGaN/GaN HEMT for future biosensing applications," *Superlattices and Microstructures*, 2021, doi:10.1016/j.spmi.2021.107086.

[24] R. Mann, et al. "Dual gate AlGaN/GaN MOS-HEMT biosensor for electrical detection of biomolecules-analytical model," Semiconductor Science and Technology, 2023, doi: 10.1088/1361-6641/acb0f3.

[25] S. Deng, et al. "High performance enhancement-mode HEMT with 3DEG to conduct current and 3DHG as back barrier," *Superlattices Microstructures*, 2019, doi: 10.1016/j.spmi.2019.04.024.

[26] K. Sehra et al., "Interplay Between γ–Ray Irradiation and 3DEG for Dosimeter Applications," *IEEE Access*, 2022, doi: 10.1109/ACCESS.2022.3155764.

[27] D. Jena, et al. "Linearity improvement in graded channel AlGaN/GaN HEMTs for high-speed applications," *Physica Scripta*, 2023, doi: 10.1088/1402-4896/acf3b6.

[28] K. Husna Hamza, et al. "Highly scaled graded channel GaN HEMT with peak drain current of 2.48 A/mm," *AEU - International Journal of Electronics and Communications, 2021*,doi: 10.1016/j.aeue.2021.153774.

[29] Topno, N., et al. "Performance characterization of Ferroelectric GaN HEMT based biosensor," *Microsystem Technology 31*, 2025, doi:10.1007/s00542-024-05727-7.

[30] S. Singh et al. "Dopingless Negative Capacitance Ferroelectric TFET for Breast Cancer Cells Detection: Design and Sensitivity Analysis," *IEEE Transactions on Ultrasonics*, 2022, doi: 10.1109/TUFFC.2021.3136099.

[31] Prabin kumar B., et al., "Performance assessment of Charge Plasma Triple Metal Gate Junctionless Vertical TFET-based Biosensor using Gate Engineering technique" Devices for Integrated Circuit (DevIC), 2025, doi: 10.1109/DevIC63749.2025.11012439.

[32] Bouguenna, A., et al., "Impact of geometrical parameters on AlGaN/GaN heterostructure MOS-HEMT biosensor" Journal of Computational Electroncs 24, 2025, doi:10.1007/s10825-024-02247-5.

[33] Prasanna, R.L., et al. "Design and performance analysis of a vertically stacked gate-all-around nanosheet FET with embedded nanocavity for biosensing applications" *Scientific Reports 16*, 2026, doi:10.1038/s41598-026-35132-1.

[34] S. Rao Karumuri, et al. "Vertically Stacked Doping-Less Dual-Metal Gate Nanosheet FET With TiO2 Dielectric for High Sensitivity Autoimmune Disease Biosensing," *IEEE Acc*ess, 2026, doi: 10.1109/ACCESS.2026.3660023.